



Virginia Commonwealth University
VCU Scholars Compass

Theses and Dissertations

Graduate School

2013

S3-S4 Linker Modulation of Voltage Sensor Relaxation in Voltage Gated Potassium Channels

W. Everett Fox

Virginia Commonwealth University

Follow this and additional works at: <http://scholarscompass.vcu.edu/etd>

 Part of the [Physiology Commons](#)

© The Author

Downloaded from

<http://scholarscompass.vcu.edu/etd/3156>

This Thesis is brought to you for free and open access by the Graduate School at VCU Scholars Compass. It has been accepted for inclusion in Theses and Dissertations by an authorized administrator of VCU Scholars Compass. For more information, please contact libcompass@vcu.edu.

**S3-S4 LINKER MODULATION OF VOLTAGE SENSOR RELAXATION IN VOLTAGE
GATED POTASSIUM CHANNELS**

A Thesis submitted in partial fulfillment of the requirements for the degree of Master of Science
at Virginia Commonwealth University.

by

WADE EVERETT FOX

BSc. University of North Carolina, Chapel Hill, NC 2011

Director: **CARLOS A. VILLALBA-GALEA, Ph.D.**

Assistant Professor

Department of Physiology and Biophysics

Virginia Commonwealth University

Richmond, Virginia

July, 2013

Acknowledgement

First and foremost, I would like to thank Dr. Carlos A .Villalba-Galea for granting me the opportunity to work for him this past year. I have greatly enjoyed his mentorship, and sincerely appreciate his guidance, support, and patience. Over the past year, Carlitos' enthusiasm and dedication for this project has furthered my own eagerness and interest in the field of research. My success in this program is due in no small part to him and his encouragement. I would also like to thank the members of my committee, Dr. Linda Boland and Dr. Clive Baumgarten for guiding me through this thesis and providing valuable insight, knowledge, and advice in shaping this project.

I would also like to thank the lab of Dr. I. Scott Ramsey and the Department of Physiology and Biophysics at Virginia Commonwealth University for providing me the materials, experience, and knowledge necessary to perform the experiments presented in this paper. Particularly, the help of Sophia Gruszecki, Mohammed Khaleduzzaman Ph.D., Kendall Hancock, Aaron Randolph Ph.D., and Heikki Vaanen without whom this project would not have been possible.

Finally, I would like to thank my parents, Jeanie and Wylie Fox, and sister, Kathryn, for their unwavering love, support, and encouragement throughout my educational career.

Table of Contents

	Page
Acknowledgements.....	iv
List of Figures.....	vii
List of Abbreviations	viii
Abstract.....	x
Chapter	
1 Background.....	1
1.1: Introduction to ion channels.....	1
1.2: Gating currents	2
1.3: Molecular basis of gating currents	3
1.4: Voltage dependence of activation is dynamic.....	5
1.5: Seeking the mechanism of VSD relaxation.....	7
1.6: The S3-S4 loops couples gating currents and relaxation	10
1.7: Hypothesis	16
2 Materials and Methods.....	17
2.1: Molecular biology	17
2.2: Electrophysiology.....	18
2.3: Analysis.....	19

3	Results.....	22
3.1:	Channel expression in proline-to-alanine mutants	22
3.2:	Kinetics of channel activation of ShakerIR and proline-to-alanine mutants	22
3.3:	Effect of the proline-to-alanine mutation on the kinetics of deactivation of Shaker	23
3.4:	Effect of the proline-to-alanine mutation on the kinetics of gating current deactivation of Shaker	25
4	Discussion and Conclusions	41
5	Final Remarks.....	47
5.1	Future directions.....	47
5.2:	On the physiological role of VSD relaxation	47
	Literature Cited	50
	Vita.....	56

List of Figures

	Page
Figure 1: Structural model of ShakerIR.....	13
Figure 2: Sequence alignments of the putative S3-S4 loop in several families of voltage gated potassium channels	14
Figure 3: Basic model for S4 segment movement during gating and VSD relaxation.....	15
Figure 4: Ionic activation currents in ShakerIR constructs.....	28
Figure 5: Kinetics of channel activation.	29
Figure 6: Ionic deactivation currents from ShakerIR and proline-to-alanine mutants	30
Figure 7: Voltage dependence of channel deactivation following relaxation.....	31
Figure 8: Deactivation current kinetics in detail.....	32
Figure 9: Relaxation voltage clamp protocol.....	33
Figure 10: Weighted average time constant of deactivation, τ_{DEACT} , following depolarizing pre-pulse of varying duration	34
Figure 11: Weighted average time constant of deactivation, τ_{DEACT} , as a function of depolarizing pre-pulse duration	35
Figure 12: Voltage sensor relaxation transition model	36
Figure 13: W434F gating current fitting	37
Figure 14: Off gating current kinetics.....	38
Figure 15: Fraction of voltage sensors in the relaxed state.....	39
Figure 16: Normalized off gating charge during relaxation	40

List of Abbreviations

A	Active State
β_1	Rate constant for the transition from intermediate (M) to resting (R) state
β_2	Rate constant for the transition from active (A) to intermediate (M) state
cDNA	Complementary DNA
cRNA	Complementary RNA
EGTA	Ethylene glycol tetra-acetic acid
f_{Q2}	Fraction of gating charge transferred during the transition from active (A) to intermediate (M) state
HEPES	4-(2-hydroxyethyl)-1-piperazineethanesulfonic acid
hERG	Human Ether-a-go-go related gene
I_{DEACT}	Ionic current of deactivation
I_{OFF}	Off gating current
M	Intermediate State
NMG	N-methyl-D-glucamine
PD	Pore domain

Q_{OFF}	Off gating charge
R	Resting State
τ_{DEACT}	Weighted time constant of deactivation
VGC	Voltage gated channel
VSD	Voltage sensing domain
VSP	Voltage sensing protein
W434F	Non-conducting Shaker channel due to mutation of tryptophan (W) to phenylalanine (F) at residue 434.

ABSTRACT

S3-S4 LINKER MODULATION OF VOLTAGE SENSOR RELAXATION IN VOLTAGE GATED POTASSIUM CHANNELS

By Wade Everett Fox, BSc.

A thesis submitted in partial fulfillment of the requirements for the degree of Master of Science
at Virginia Commonwealth University.

Virginia Commonwealth University, 2013.

Major Director: Carlos A. Villalba-Galea, PhD.
Assistant Professor
Department of Physiology and Biophysics

It is commonly assumed that the voltage dependence for activation of voltage-gated channels is an intrinsic characteristic of the protein that remains unchanged during electrical activity. However, sporadic reports have suggested otherwise by showing that voltage dependence changes in a use-dependent manner resulting in a voltage dependence shift towards negative potentials (Bezanilla et al., 1982; Bruening-Wright and Larsson, 2007; Kuzmenkin et al., 2004; Labro et al., 2012; Larsson and Elinder, 2000; Olcese et al., 1997; Piper et al., 2003; Shirokov et al., 1992). Although the mechanism underlying the shift in voltage dependence

remains unclear, this process seems to have two components. The first stage has been proposed to be related to the stabilization of the open conformation of the pore domain (Labro et al., 2012). The second stage seems to involve the stabilization of the activated state of the voltage sensing domain (VSD) (Labro et al., 2012; Lacroix et al., 2011) through a process known as VSD relaxation (Villalba-Galea, 2012; Villalba-Galea et al., 2008). This latter process has been proposed to be an intrinsic property of the VSD in which the domain is stabilized in an active-like state referred to as the relaxed state. Yet, the underlying mechanism remains unknown. This project expands upon the hypothesis that the movement of the fourth transmembrane (S4) segment of the VSD can induce conformational changes using the loop connecting the third and fourth transmembrane segments (S3-S4 loop) to couple VSD activation to VSD relaxation. Using the *Drosophila* potassium-selective, voltage-gated channel *Shaker* as a model, I show here that mutations in the S3-S4 loop of the VSD modulate the time constant of deactivation of the conductance and cause an apparent partial immobilization of the sensing charges of the VSD. These results hint, for the first time, at a mechanism for VSD relaxation. Particularly, these results indicate that the S3-S4 loop is intimately involved in the mechanism of coupling VSD activation to VSD relaxation.

Background

1.1: Introduction to ion channels

The research conducted by Alan L. Hodgkin and Andrew F. Huxley on the basis for the generation of action potentials paved the way for the modern-day understanding of the molecular basis for electrical signaling in excitable cells (Hodgkin and Huxley, 1952a; Hodgkin and Huxley, 1952b). From their seminal work, Hodgkin and Huxley concluded that the electrical activity in excitable cells is caused by the flow of ions, such as sodium and potassium, through an ion-selective “conductive pathway”, whose conduction is controlled by the membrane potential. Furthermore, they also proposed that “charged particles” associated with the conduction pathways in the membrane confer voltage dependence to the activity of these pathways. Today, the molecular identity of the “conduction pathways” and the “charged particles” predicted by Hodgkin and Huxley have been well established. Both functional entities are constituted by membrane-embedded proteins, known as voltage-gated channels. Structurally, the “conduction pathways” are formed by the pore domain of these proteins; the “charged particles” are represented by charged amino acid residues within the hydrophobic, membrane-embedded core of these proteins (Long et al., 2005a; Long et al., 2007; Noda et al., 1984; Swartz, 2008; Tempel et al., 1987).

Voltage-gated ion channels are complex transmembrane proteins composed of a central ion-permeable pore surrounded by four voltage-sensing domains in a radially symmetric arrangement. In particular, voltage-gated potassium channels are tetrameric proteins composed of six transmembrane segments. The first four transmembrane segments (S1-S4) form a domain known as the voltage sensing domain (VSD); the last two segments, S5-S6, form the pore domain (PD) (Long et al., 2005a; Long et al., 2007) (Fig. 1). The VSD contains charged residues that are responsive to the difference in electrical potential across the membrane. These residues can drive conformational changes within the VSD that, in turn, can be transmitted to the PD, controlling its activity. The coupling between the VSD and the PD constitutes the basic mechanism that confers voltage dependence to the conductance in this type of channel.

1.2: Gating currents

Hodgkin and Huxley speculated in their early work that the activation of the voltage-controlled, ion selective conductances was the result of “particles” reaching a specific conformation in the membrane (Hodgkin and Huxley, 1952b). Because the movement of these particles was induced by changes in membrane potential, it was expected that a finite charge would be associated to them. Thus, the movement of charged particles will produce a transient current. The first direct evidence demonstrating the existence of charges emerged in the early 1970s. At that time, it was shown that depolarization of the membrane of the giant squid axon produced a small outward current

in the absence of permeable ions (Armstrong and Bezanilla, 1973; Bezanilla and Armstrong, 1974; Keynes and Rojas, 1973). These currents were intrinsic of the conduction pathway and were, therefore, called gating currents since they were attributed to the opening (activation) and closing (deactivation) of the sodium channels (Keynes and Rojas, 1973). Today, a wealth of experimental results has demonstrated that charged residues residing within the hydrophobic core of the VSD confer voltage-dependence to the activity of voltage-sensing proteins such as Na⁺ channels, K⁺ channels, voltage sensitive phosphatases and others membrane-embedded proteins (Bezanilla, 2008b).

1.3: Molecular basis of gating currents

During depolarization, the VSD undergoes electrically driven conformational changes that are transmitted to the PD leading to its opening (Bezanilla, 2008a). Charged residues of the VSD, such as positive arginine and negative aspartate, may function as sensing particles that confer voltage sensitivity to this domain (Bezanilla, 2008a). Those charges that effectively sense the electrical field are commonly referred to as gating (or sensing) charges. Thus, the residues carrying these gating charges are dubbed as gating charge residues. In general, the main gating charge residues are located in the fourth (S4) segment of the VSD. When the magnitude and polarity of the electrical field is changed, the position of the gating charges also changes. This voltage-dependent movement of the gating charges ultimately leads to conformational changes in the S4 segment, thus conferring a voltage sensitivity to the channel protein (Bezanilla, 2005; Bezanilla, 2008a;

Swartz, 2008). The S4 segment is mechanically coupled to the pore domain through the S4-S5 linker. Following depolarization, the electrically-driven movement of the S4 segments is transmitted to the PD domain through the S4-S5 linker (Bezanilla, 2008a; Long et al., 2005b). This electro-mechanical coupling constitutes the main mechanism conferring voltage control of the opening and closing of the PD. Since the VSD controls the activity of channels, investigating the molecular basis for the functioning of this domain is essential to obtain a comprehensive understanding of the mechanism for generation and control of electrical activity in cells.

The voltage sensing current is a transient current resulting from the movement of the charges in response to electrical field changes. In voltage-gated channels, this sensing current is involved in the process that opens and closes the pore, or “gate”, necessary for ionic current conductance (Bezanilla, 2005; Bezanilla, 2008b; Tombola et al., 2006). Therefore, the voltage sensing current is referred to as the gating current in voltage-gated channels since it is necessary for the transition from the open-to-closed state and the closed-to-open state.

In voltage-gated potassium channels *Shaker*, the gating current event has been proposed to be the sum of a shot-like movement, where charge is carried in “discrete packages” (Bezanilla, 2000; Sigg et al., 1994). During membrane depolarization resulting in the transition from the deactivated state to the activated state, the movement of the gating charges is to discrete positions rather than gradual movement, producing an outward gating current. These currents are referred to as the “ON” gating currents due to

the fact that the channel becomes activated. Similarly, during membrane repolarization and the transition from the activated state to the deactivated state, an inward gating current is produced. These are known as the “OFF” gating currents.

In *Shaker*, the charge movement associated with channel gating is approximately 13 elementary charges (e_0) (Schoppa et al., 1992). Since the channel is formed by four subunits, the movement of 13 e_0 during channel gating suggests that each VSD contributes three charges to the gating. Therefore, four charged residues are involved in gating. The channel does not fully open until all thirteen charges have moved, indicating that channel opening is dependent on the concerted movement of all four VSDs to the activated state (Perozo et al., 1993; Seoh et al., 1996; Tempel et al., 1987). The first four arginines, R362, R365, R368, and R371, have been shown by charge neutralization mutations to contribute to the main gating charge (Aggarwal and MacKinnon, 1996; Seoh et al., 1996).

1.4: Voltage dependence of activation is dynamic

Since the time of Hodgkin and Huxley, it has been assumed that the voltage dependence of the conductance remained unaltered during electrical activity. However, this view began to change in the early 1980s when Bezanilla and colleagues showed that following prolonged depolarization in the giant squid axon, the voltage dependence of gating currents associated with Na^+ conductance shifted to more negative potentials (Bezanilla et al., 1982). These observations illustrated for the first time that voltage

dependence of voltage-gated channels is likely dynamic. In the case of *Shaker*, voltage dependence of gating currents recorded from this channel shifted between -15 mV and -25 mV when the membrane potential was held at 0 mV (Labro et al., 2012; Lacroix et al., 2011; Olcese et al., 1997). To date, voltage dependence shift has been described in a number of voltage-controlled proteins, including the bacterial sodium channels (Kuzmenkin et al., 2004), L-type calcium channels (Shirokov et al., 1998), hERG channels (Piper et al., 2003), HCN channel family (Larsson and Elinder, 2000), the voltage phosphatase Ci-VSP (Villalba-Galea et al., 2008), and the genetically-encoded membrane potential probe VSFP 2.3 (Akemann et al., 2009; Villalba-Galea et al., 2009a).

No mechanisms have been ascribed to the shift in voltage dependence. However, in the case of the squid Na^+ channels and *Shaker*, the changes in voltage dependence were attributed to the inactivation of the channels (Bezanilla et al., 1982; Olcese et al., 1997). Particularly, it was thought that the inactivation of the conductance was rendered by the transition of the channel into a stable conformation. Thus, deactivation of the channel must overcome the stabilized, inactivated states of these channels (Haddad and Blunck, 2011; Larsson and Elinder, 2000; Olcese et al., 1997). Similar interpretations have been offered to explain the shift in voltage dependence observed in Na^+ channels (Bezanilla et al., 1982), Ca^{2+} channels (Shirokov et al., 1998; Shirokov et al., 1992), and hERG (Piper et al., 2003).

More recently, it was shown that the VSD of voltage sensitive phosphatase (VSP) isolated from the tunicate *Ciona intestinalis* shifts its voltage dependence for charge

movement upon prolonged activation (Villalba-Galea et al., 2008). This process, named VSD relaxation, was shown to be intrinsic of the VSD, since this phosphatase, known as Ci-VSP, does not have a pore domain. This observation indicated for the first time that the inactivation of the pore may not be required for shifting the voltage dependence of charge movement in voltage-gated channels (Villalba-Galea et al., 2008). Since then, new evidence has emerged in the literature indicating that VSD relaxation may partially account for changes in the deactivation kinetics of *Shaker* (Labro et al., 2012; Lacroix and Bezanilla, 2011). Furthermore, introduction of a mutation that partially abolished C-type inactivation failed to prevent these changes in *Shaker* (Labro et al., 2012), indicating that stabilization of the active state of the VSD by the pore may not be the cause for them.

1.5: Seeking the mechanism of VSD relaxation

VSD relaxation was first described in a voltage sensitive phosphatase isolated from the tunicate *Ciona intestinalis* (Villalba-Galea et al., 2008). This enzyme, commonly referred to as Ci-VSP, is a phosphoinositide phosphatase (Halaszovich et al., 2009; Kurokawa et al., 2012; Murata et al., 2005; Murata and Okamura, 2007) with catalytic activity under the control of a VSD resembling those found in voltage gated channels (Villalba-Galea, 2012). This enzyme does not have a pore domain. Instead, the C-terminus of Ci-VSP forms an intracellular cellular catalytic domain. Persistent activation of the VSD of Ci-VSP causes a shift in the voltage dependence for sensing

charge movement, even in constructs in which the catalytic domain has been deleted (Villalba-Galea et al., 2008) or replaced by other molecular entities (Akemann et al., 2009; Villalba-Galea et al., 2009b). These observations have demonstrated that relaxation, at least in this enzyme, is an intrinsic property of the VSD. The mechanism for VSD relaxation remains unknown. Yet, it has been shown that VSD relaxation is likely a voltage-independent process consisting of a transition from the active state of the VSD, reached after depolarization, to a “lower energy” state (Villalba-Galea, 2012).

In the original description of the phenomenon, it was proposed that VSD relaxation was a “local” event involving a putative transition from a “long, thin, tightly-wound” 3_{10} helix to a “short, thick, and more stable α -helix” of the S4 segment following activation of the VSD (Vieira-Pires and Morais-Cabral, 2010; Villalba-Galea, 2012; Villalba-Galea et al., 2008) (Fig. 3). However, more recently it has been proposed that VSD relaxation may be the consequence of a rearrangement involving other segments of the VSD, and a “global” phenomenon (Villalba-Galea, 2012). To understand this idea, consider that, at negative potentials, the VSD segments S1 to S3 likely accommodate the S4 segment in a “low energy” state (resting state) (Fig. 3). Changing to positive potentials drives the movement of sensing charges associated with the S4 segment that, in turn, produce gating (or sensing) currents. During the rapid movement of the S4 segment, the VSD gains potential energy from the work done by the electric field on the sensing charges. If the return of sensing charges starts following a short-lived activation, voltage dependence may remain unaltered. In contrast, if the activation of the VSD is prolonged,

a conformational change in the VSD may be driven by the potential energy gained from the work done by the electrical field on the sensing charges. In this case, the conformational rearrangement will dissipate energy. Hence, compensation for the dissipated energy during VSD remodeling is required to return the VSD to the resting state. Since the source of energy is the difference in electric potential across the membrane, then this additional energy cost is observed as a shift to negative potentials in the voltage dependence.

In the aforementioned view, activation and relaxation are processes of different natures. The former consists of an electrically-driven, rapid displacement of the S4 segment that leads the VSD into a “higher energy” conformation. The latter, relaxation, is driven by the potential energy gained by the VSD during the activating movement. In this view, the shift observed in voltage dependence is the consequence of a process taking place within the VSD rather than in the pore, where relaxation stabilizes the active state of the VSD.

Because the voltage dependence of voltage-gated channels is conferred by the VSD, relaxation may be the consequence of conformational changes within the voltage sensor. It has been proposed that relaxation is intimately related to slow inactivation of the conduction, also known as C-type inactivation (Haddad and Blunck, 2011; Larsson and Elinder, 2000; Olcese et al., 1997). However, it has been shown that relaxation is also a phenomenon involving the voltage sensor and that relaxation is independent of C-type inactivation (Labro et al., 2012). During a depolarizing pre-pulse, the time constants of

deactivation for gating and ionic currents demonstrate a biphasic nature as a function of pre-pulse duration (Labro et al., 2012). The proposed explanation for this biphasic nature is two stages involving the pore and relaxation separately. As the membrane depolarizes during the pre-pulse, the channel transitions from the closed state to the open state. The initial slowing of deactivation is attributed to the stabilization of the bundle-crossing gate during this closed-to-open transition. If this depolarization is maintained, typically greater than 200 ms, then the voltage sensor will undergo an additional stabilization called the open relaxed state (Labro et al., 2012). This VSD stabilization accounts for the second stage of slowing of deactivation. The proposed model indicates four distinct states. During a stimulating depolarization, the voltage sensor transitions from a resting state to an active state. The longer the depolarization stimulus experienced by the membrane, the greater the population of VSDs in the active conformation.

1.6: The S3-S4 loops couples gating currents and relaxation

We sought to investigate the molecular mechanism for relaxation. We argue that relaxation is triggered by the persistence of the S4 segments of the VSD in the active position. It is possible the sudden movement of the S4 segment during activation causes a distortion in the VSD that displays resilience. However, prolonging the lifespan of the active state by persistent depolarization may trigger the remodeling of the VSD to accommodate the new position of the S4 segment. The S4 segment and the rest of the VSD are directly connected through the S3-S4 loop. Deletion mutations of this loop

showed a periodicity of seven amino acids per turn, which is characteristic of a helical conformation, which may give it some rigidity (Gonzalez et al., 2001). Partial deletion of the S3-S4 slows down the kinetics of deactivation and activation in *Shaker* channels (Gonzalez et al., 2000; Gonzalez et al., 2001; Tabarean and Morris, 2002), consistent with the idea that the S3-S4 loop is able to influence the dynamics of the S4 segment and the VSD in general. Following this idea, we argue that the energy gained by the VSD when mechanical work is done on the S4 segment by the electrical field across the membrane may be transmitted from the S4 segment to the rest of the VSD via the S3-S4 loop. Therefore, we propose that the S3-S4 loop is critical for VSD relaxation.

Relaxation is triggered following sustained activation of the VSD. Thus, the displacement of the fourth (S4) segment towards the extracellular side of the membrane is likely to trigger this process. In terms of the thermodynamics of this process, the movement of the S4 segment can be seen as the gain of energy by the VSD from the work done on the S4 segment by the electrical field. It has been proposed that the gained energy is eventually dissipated and therefore, a larger change in potential – the source of energy for this process – is required to drive the S4 segment back to its initial position. Here, we propose that the flexible voltage sensor linker region, the S3-S4 loop, plays a role in the relaxation kinetics by acting as a “transmission line” of electromechanical work between the S4 voltage sensor segment and the rest of the VSD. It is observed from sequence alignments of voltage-gated potassium channels that proline residues are conserved in several S3-S4 linkers. We hypothesize that the three proline residues within

the *Shaker* S3-S4 linker region may play a role in relaxation by acting as helix-breaking “hinges” to reduce the transmission of energy between the S3 and S4 segment. To test this hypothesis, we created mutations in which the three prolines were individually exchanged to alanine. Then, using cut-open voltage clamp, the macroscopic and gating currents were measured in *Xenopus* oocytes to observe the effect of each proline-to-alanine construct on channel activation, channel deactivation after prolonged depolarization, and gating current deactivation after prolonged depolarization.

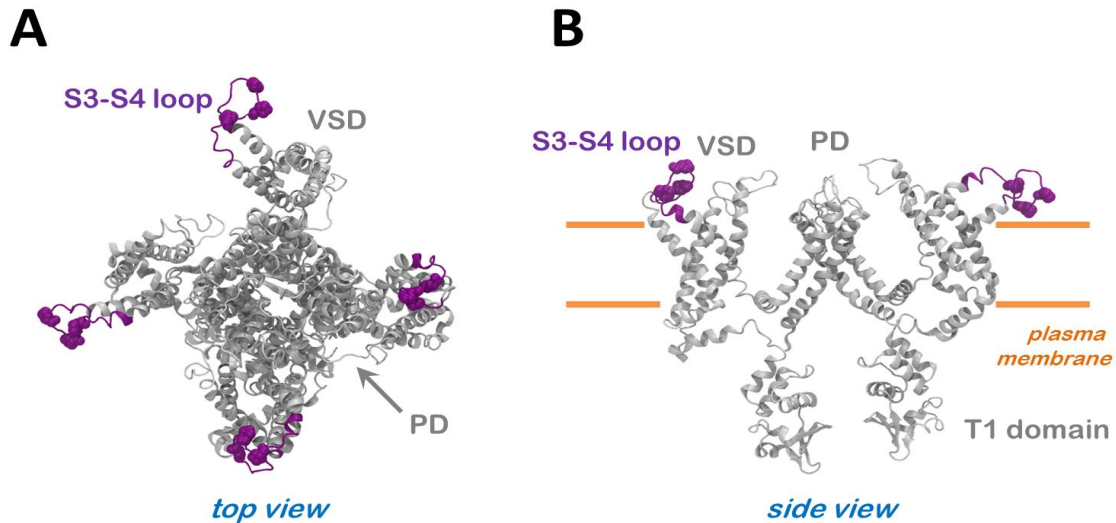


Figure 1. Structural model of ShakerIR in the activated state. Kindly provided by Dr. Fatemeh Khalili-Araghi (University of Illinois at Urbana Champaign). The model was built with the package “Modeller” using the structure of the chimeric potassium selective, voltage-gated channel Kv1.2-Kv2.1 (Long et al., 2007). A) Top view of the structure displaying the central pore domain (PD) surrounded by four voltage sensing domains (VSD). The S3-S4 loops are shown in purple and the 3 proline residues present in this region are shown as van der Waals spheres. B) Side view of two of the four subunits in the structure shown in A. The orange lines represent the position of the head-groups of phospholipids in the membrane.

	<i>S3-S4 loop</i>	
Shaker	PYFITLATVVAEEEDTLNLPKAPVSPQDKSSNQAMSLAILR	362
hKv1.1	PYFITLGTEIAEQ-----EGNQKGEQATSLAILR	292
hKv1.2	PYFITLGTELAKEP-----EDAQQGQQAMSLAILR	294
hKv1.3	PYFITLGTELAER-----QGNGQQAMSLAILR	364
hKv1.4	PYFITLGTDLAQQQG-----GGNGQQQQAMSFALR	444
hKv1.5	PYFITLGTELAEEQPG-----GGGGGQNGQQAMSLAILR	400
hKv1.6	PYFITLGTELVQQQEQQ----PASGGGGQNGQQAMSLAILR	342
hKv1.7	PYFVALGTELARQ-----RGVGQQAMSLAILR	278
hKv2.1	PYYVTIFLTESNKS-----VLQFQNVRRVVQ	297
hKv2.2	PYYVTIFLTESNKS-----VLQFQNVRRVVQ	301
hKv3.1	PFYLEVGLSGLSS-----KAAKDVLGFLR	311
hKv3.2a	PFYLEVGLSGLSS-----KAAKDVLGFLR	348
hKv3.3	PFYLEVGLSGLSS-----KAAKDVLGFLR	414
hKv3.4	PFYLEVGLSGLSS-----KAARDVLGFLR	347
hKv4.1	PYYIGLLVPKNDD-----VSGAFV	296
hKv4.2	PYYIGLVMTDNED-----VSGAFV	294
hKv5.1	PFYVSLTLTHLGAR-----MMELTNVQQAVQ	290
hKv6.1	PYYITLLVDGAAAGRRK-----PGAGNSYLDKVGVLVR	343
hKv6.2	PFYVSLLLG-LAAG-----PG-GTKLLERAGLVR	288
hKv7.1	ASMVLCVGSKGQ-----VFATSALR	230
hKv7.2	ASIAVLAAGSQGN-----VFATSALR	200
hKv7.3	ASVPVAVGNQGN-----VLATS-LR	230
hKv7.4	ASVAVIAAGTQGN-----IFATSALR	206
hKv7.5	ASIAVSAKTQGN-----IFATSALR	234

Figure 2. Sequence alignments of the putative S3-S4 loop in several families of voltage gated potassium channels. As shown here, the S3-S4 loop displays high variability among different families of these channels, making this region an attractive target for developing pharmacological agents. Proline residues can be found in the S3-S4 loops of Shaker, Kv1.2, Kv1.5, Kv1.6, Kv6.1, and Kv6.2.

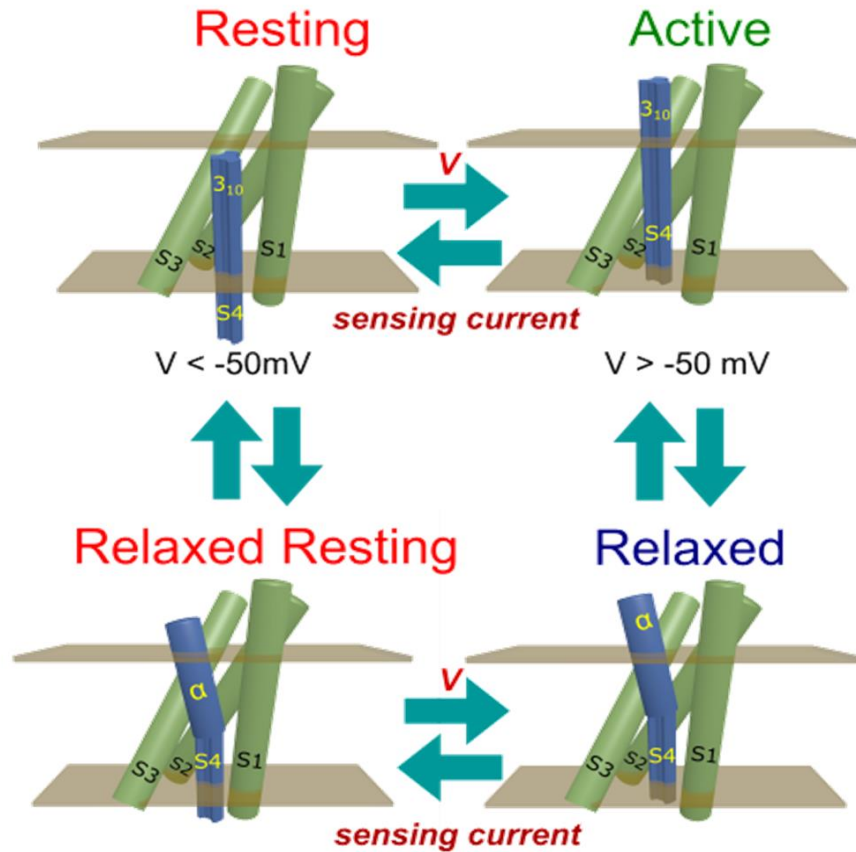


Figure 3. Basic model for S4 segment movement during gating and VSD relaxation. The S4 segment is thought to be the main carrier of gating charges in the VSD. Found in the resting state at negative potentials (top left), the S4 segment moves towards the extracellular space driven by a change of the membrane potential to more positive voltages reaching the activated state. If the depolarization is prolonged, the S4 segment will transition to the relaxed state. It has been proposed by Villalba-Galea and colleagues that the transition of the S4 segment from the active to the relaxed state involves a structural conformation change of the S4 from a 3_{10} to an α -helix (Villalba-Galea et al., 2008). During this transition, the voltage dependence for the movement of gating charges is shifted to more negative potentials. This shift may be the consequence of dissipation of the energy gained by the work done by the electric field on the gating charges of the VSD.

1.7 Hypothesis

Following activation, S4-based voltage sensing domains (VSD) undergo a voltage independent transition, VSD relaxation, shifting their voltage dependence to more negative potentials. Since relaxation is seemingly an intrinsic property of VSDs, we sought to identify regions of the domain involved in the triggering of relaxation. For this, we focused our study on the S3-S4 loop. We argue that, like the S4-S5 linker coupling the VSD to the pore domain, the S4 segment can do electromechanical work on the rest of the VSD using the S3-S4 loop as a “coupling element”. Several studies have proposed that the S3-S4 is folded in an α -helix. Hence, we hypothesized that the movement of the S4 segments can be readily transmitted to the S3 segment and the rest of the VSD causing relaxation through a “rigid” S3-S4 loop. Conversely, a “flexible” S3-S4 would be able to absorb the movement of the S4 segment, dissipating mechanical energy and diminishing relaxation. To test this idea, we determined amplitude and timing of relaxation by performing cut-open voltage-clamp recordings of potassium currents from *ShakerIR* S3-S4 loop proline-to-alanine mutants. We reason that, since prolines disrupt helical structure, introduction of a “helix-friendly” alanine will increase the rigidity of the loop. Hence, we proposed that S3-S4 loop’s prolines act as “hinges” conferring flexibility to this region.

Materials and Methods

2.1: Molecular biology

The vector pBSTA containing *Shaker*IR was received as a gift from Dr. Francisco Bezanilla (University of Chicago). Mutation of prolines 341, 344, and 347 to alanine was done using a PCR site-directed mutagenesis technique. Oligonucleotides containing the desired mutation were used to prime the chain reaction. XL-Blue (Stratagene) competent cells were transformed with the PCR product. Plasmids were isolated from the bacteria culture by lysis and cDNA isolation using a resin-based technique, or Miniprep (Qiagen). Mutations were confirmed by commercial sequencing (Genewiz).

For cRNA synthesis, cDNA was linearized with NotI. For expression of *Shaker*, cRNA was synthesized in vitro using the mMESSAGE mMachinE T7 (Ambion, Invitrogen). *Xenopus* oocytes injected with 2-25 ng of cRNA were incubated under standard conditions for 24-72 hours (Labro et al., 2012).

2.2: Electrophysiology

Electrophysiological recordings were performed using a custom-made package programmed in LabVIEW (National Instruments) by Dr. Villalba-Galea. The package, named “JustAcquire”, controlled an acquisition board NI USB-6221 (National Instruments). Current recordings were digitalized at 250 kHz, following analogical filtering at 20-100 kHz. The data was oversampled at 5-25 kHz for storage and offline analysis. The data was analyzed using a custom-made program written in Java (Oracle Corp.) by Dr. Villalba-Galea and with Origin 9.0 (OriginLab).

Ionic and gating currents were measured utilizing the cut-open voltage clamp technique (Taglialatela et al., 1992). Oocytes were placed in a 3-chamber cut-open setup and their bottom membranes permeabilized with internal solution (see below) containing 1-2% saponin. For the ionic current recordings, the extracellular solution was made of (in mM) 12 KOH, 88 N-methyl-D-glutamine (NMG), 90 Methanesulfonic acid (MeSO₃), 10 HEPES, and 2 Ca²⁺ at a pH of 7.4. The intracellular solution was made of (in mM) 100 KOH, 90 MeSO₃, 10 HEPES, 2 EGTA at pH 7.4. For gating current recording, *Xenopus* oocytes injected with cRNA of *ShakerIR* carrying the mutation W434F (Perozo et al., 1993) which renders channels that do not produce measurable ionic currents. The recording solutions were made of (in mM) 100 NMG, 90 Methanesulfonic acid (MeSO₃), 10 HEPES, and 2 Ca²⁺ for the external solution, and 2 mM EGTA for the internal solution at pH 7.4.

2.3: Analysis

The deactivation of ionic currents was best described by a double exponential function as shown elsewhere (Labro et al., 2012; Lacroix and Bezanilla, 2012). The double exponential function was defined as follows,

$$I(t) = I_1 e^{\left(-\frac{t}{\tau_1}\right)} + I_2 e^{\left(-\frac{t}{\tau_2}\right)} + I_{LEAK}$$

Where τ_1 and τ_2 are the time constants associated with each component, I_{LEAK} is the amplitude of the leak current, and I_1 and I_2 are the amplitudes of each of these components. The time constant of ionic current deactivation (τ_{DEACT}) was defined as the weighted average time constant from the fit. The weighted average was calculated as follows,

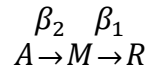
$$\tau_{DEACT} = \frac{I_1 \tau_1 + I_2 \tau_2}{I_1 + I_2}$$

The τ_{DEACT} values were plotted with respect to the deactivating potential. A graph of τ_{DEACT} at a membrane potential of -60 mV versus pre-pulse duration was created to simply illustrate the increase in the deactivation time constant as a function of increasing pre-pulse duration.

To characterize the effect of the proline-to-alanine mutations on the VSD activity, the net gating charge (Q) versus potential (V) curves were generated by numerical integration of the gating currents. In this case, mutant W434F (Perozo et al., 1993) was

used to measure gating current to avoid the masking of gating current by the potassium conductance.

The kinetics of deactivation of the VSD was determined from gating currents recorded following a pulse to +40 mV. Following the paradigm established by Labro and colleagues (Labro et al., 2012), deactivating (OFF) gating currents were recorded at -70 mV, following an activating pulse to +40 mV. To characterize the effect of the proline-to-alanine mutations on VSD relaxation, the duration of the activating pulse was varied between 0.5 and 8192 ms in an exponential scale. Since the currents displayed a sigmoidal behavior in time, it was assumed that the deactivation of the VSD occurred in at least two steps. Following this idea, a three-state model was used to kinetically characterize OFF-gating currents. Assuming that at -70 mV the deactivation of the VSD is practically irreversible, the transition of the VSD from the active (*A*) to the resting (*R*) state occurred through an intermediate state (*M*). Thus, the kinetic scheme will be



Where β_2 and β_1 are voltage-dependent rate constants for the transitions from *A* to *M* and *M* to *R*, respectively. The OFF-gating currents will be described by the equation,

$$I_{OFF} = Q_{MAX}(f_2\beta_2A + (1 - f_2)\beta_1M)$$

where Q_{MAX} is the total gating charge in the entire population of VSD and f_2 is the fraction of the Q_{MAX} associated to each of the first transition. The differential equations describing this system above are,

$$\frac{dA}{dt} = -\beta_2 A$$

$$\frac{dM}{dt} = \beta_2 A - \beta_1 M$$

$$\frac{dR}{dt} = \beta_1 M$$

Using Maple (version 17, Maplesoft), this system of differential equations was solved.

The solutions for A and M are:

$$A(t) = e^{-\beta_2 t}$$

$$M(t) = \frac{\beta_2}{\beta_1 - \beta_2} (e^{-\beta_2 t} - e^{-\beta_1 t})$$

Thus, the equation describing the OFF-gating current had the following form:

$$I_{OFF}(t) = Q_{MAX} \left(f_2 \beta_2 e^{-\beta_2 t} + (1 - f_2) \frac{\beta_1 \beta_2}{\beta_1 - \beta_2} (e^{-\beta_2 t} - e^{-\beta_1 t}) \right)$$

This equation described the time course of OFF-gating currents before VSD relaxation.

To characterize relaxation it was assumed that a transition between the non-relaxed and relaxed modes of the VSD was slow enough that non-relaxed and relaxed VSDs could be treated as independent populations. Thus, for the relaxed I_{OFF} , an equation as described above was used. Finally, each recording was fitted to a double I_{OFF} function defined as follows

$$I_{OFF} = Q_{MAX}(1 - F) * I_{OFF,non-relaxed} + F * I_{OFF,relaxed}$$

Where F is the fraction of the population of VSD that are relaxed.

Results

3.1: Channel expression in proline-to-alanine mutants

Using the cut-open voltage clamp technique, ionic currents from oocytes expressing the constructs *ShakerIR* and mutants P341A, P344A, and P347A were recorded. The mutants were functional as evidenced by the presence of robust conductance (Fig. 4). The amplitude and kinetics of the currents recorded for the mutant channels resemble those observed from the background construct, *ShakerIR*. This observation suggested that the mutations had no effect on the activity of the channels. .

3.2: Kinetics of channel activation of *ShakerIR* and proline-to-alanine mutants

The conductance of the proline-to-alanine mutants were voltage dependent, activating at membrane potentials above -45 mV (Fig. 5A). To compare the activation of the mutants with respect to *ShakerIR*, the average normalized amplitude at the end of a 50 ms activation pulse was plotted with respect to membrane potential. As shown in Figure 5B, all of the plots overlap indicating that voltage dependence is unaltered by the

mutation. To extend this analysis, the time constant of activation was also determined by fitting to a double exponential function. The weighted average time constant vs. membrane potential (τ -V) curves show no difference between *ShakerIR* and the mutants (Fig 5C). Thus, it is concluded that replacing the prolines of the S3-S4 loop for alanine has no effect of the activation of the channels.

3.3: Effect of the proline-to-alanine mutation on the kinetics of deactivation of Shaker

Having shown that the activation of the channels is unaffected by proline-to-alanine mutations in the S3-S4 segment, the attention was turned to the deactivation process. To do so, the voltage dependence of deactivation was assessed by recording the ionic current at potentials ranging from -140 mV to +20 mV following an activating pulse to +40 mV lasting 5000 ms. In contrast to what was observed for the activation, the kinetics of deactivation seem to be slower for the proline-to-alanine mutants when compared to *ShakerIR* (Figure 6). When the constructs were depolarized to +40 mV for 1000 ms, then deactivated from -160 mV to +40 mV, the voltage dependence of deactivation did not appear to change (Fig. 7). Detailed inspection of the recording seems to confirm this idea (Fig. 8). To quantify the effect of the mutations on the kinetics of deactivation of the ionic currents, the weighted time constant of channel closure after a prolonged depolarization was calculated, following the paradigm established by Labro and colleagues (Labro et al., 2012) (Fig. 9). Briefly, the deactivation kinetics of the ionic

currents were quantified by fitting the current traces to a double exponential function, and the weighted average time constant was used to assess the kinetics. In addition, the duration of the activating pulse was varied to explore the time dependency of the slowdown of the kinetics of deactivation as a function of time (Fig. 9). As it has been shown before, there is a biphasic slowing down of the deactivating current (I_{DEACT}) following a prolonged membrane depolarization. As the duration of the activating pulse increases, the kinetics of deactivation become slower. As it has been reported, the fast phase of I_{DEACT} slowing is attributed to the stabilization of the open pore during channel activation, while the slow phase of I_{DEACT} is associated with the process of relaxation.

As shown in Figure 10, the τ_{DEACT} for +40 mV pre-pulses of duration between 10 ms and 10 s was plotted versus membrane potential. For both *ShakerIR* and the proline-to-alanine mutants, as the activation was held for longer durations, the τ_{DEACT} increased. To characterize the effect of pre-pulse duration on the deactivation kinetics, τ_{DEACT} obtained from recordings at -60 mV was plotted against the duration of the pre-pulse (τ_{DEACT} -t curve) (Figure 11). The deactivation currents of *ShakerIR* and each of the mutants at -60mV following the deactivating pulse. The τ_{DEACT} -t plots illustrate a biphasic curve, similar to those previously illustrated (Labro et al., 2012), the first phase with the fastest deactivation time constant is related to the stabilization of the open pore conformation; the phase with the slowest time constants are related to the VSD relaxation (Labro et al., 2012; Lacroix et al., 2011). The τ_{DEACT} for *ShakerIR* and each of the proline-to-alanine mutants are fast and nearly identical for a pre-pulse lasting less than 200 ms ($p < 0.05$). In

contrast, for pre-pulses longer than 500 ms, the deactivation became slower for the mutants with respect to *ShakerIR* ($p < 0.05$). The τ_{DEACT} for the mutants, however, is much slower at longer pre-pulse durations than the τ_{DEACT} for *ShakerIR*. These data suggest that at pre-pulse durations greater than 500ms, the proline-to-alanine mutants have a much slower τ_{DEACT} .

3.4: Effect of the proline-to-alanine mutation on the kinetics of gating current deactivation of Shaker

Labro and colleagues also correlated the gating current kinetics to ionic current kinetics as a function of depolarization duration (Labro et al., 2012). The I_{OFF} exhibited a biphasic slowing down with both a fast and slow phase as the time of membrane depolarization increased. The fast phase I_{OFF} slow-down was shown to be associated with stabilization of the VSD due to pore opening (Batulan et al., 2010; Kanevsky and Aldrich, 1999), while the slow phase of I_{OFF} slow-down was associated with the process of VSD relaxation (Lacroix et al., 2011).

Using the mutant *ShakerIR* W434F as a background construct, the effect of proline-to-alanine mutations of I_{OFF} was evaluated following the same relaxation protocols used for ionic currents. To characterize the kinetics of the I_{OFF} , the current traces were fitted to a double I_{OFF} equation, one representing the fraction of non-relaxed VSDs and the other representing the relaxed VSDs (Methods section and Fig. 12). The I_{OFF} current traces were well-fitted to the equation as shown in Figure 13. Three key

parameters define the kinetics of I_{OFF} according to this model. Those parameters are β_2 , β_1 , and f_{Q2} which are the rate constants for the transition from A to M, the rate constant for the transition from M to R, and the fraction of the gating charge transferred during the transition between A to M. For the non-relaxed sensors, the fitted parameter revealed that the first transition was faster for the mutants P344A and P347A but not for the mutating P341A with respect to *ShakerIR* ($p < 0.05$) (Fig. 14A). However, the fraction of the charge mobilized during the first transition was four-fold higher for the mutant P341A and two-fold for the mutant P344A in comparison to *ShakerIR* ($p < 0.05$) (Fig 14C). This suggests that the initial deactivation of the VSD is affected by the mutation P341A and P344A. In the case of the relaxed sensor, no changes in the kinetics parameter were observed ($p < 0.09$, $p < 0.14$, $p < 0.39$, for β_{21} , β_{22} , and f_{22} , respectively). This observation seems paradoxical considering the effect of the proline-to-alanine mutations on the kinetics of deactivation of ionic currents. The second transition was not different for any of the mutants with respect to *ShakerIR*. In general, both rate constants were smaller than those observed for non-relaxed mutants and the charge was mobilized mainly during the second transition (Fig. 14B). This indicates that the electrical characteristics of the VSD may have changed during relaxation.

The fraction of VSDs in the relaxed state was analyzed as a function of the initial depolarizing pulse duration (Fig. 15). As this depolarizing pulse duration increased from 10 ms to 10 s, the fraction of voltage sensors in the relaxed state increased. Interestingly, only the proline-to-alanine mutation at position 341 lead to an increased number of

voltage sensors in the relaxed state compared to the background construct. The mutations at positions 344 and 347 did not have any observable differences compared to the background construct. Again, this is contradictory to our previous data illustrating the effect of proline-to-alanine mutations on the kinetics of deactivation of ionic currents after prolonged depolarization.

Since the movement of the charges was restricted to the second transition of the sensor, it is arguable that the first transition constitutes a rate-limiting state of the generation of I_{OFF} . Furthermore, our data argue that the magnitude of the rate is approximately 0.025 ms^{-1} . This means that charges becomes “available” for movement with a time constant of 40 ms. Therefore, it is expected that a fraction of I_{OFF} is too slow to be resolved. To address this hypothesis, OFF-gating charges (Q_{OFF}) were calculated by numerical integration of I_{OFF} over a period of 300 ms as a function of the activating pulse duration. As shown in Figure 16, Q_{OFF} for *ShakerIR* decreased merely 2% after a pulse to +40 mV for over 8000 ms. In contrast, all of the proline-to-alanine mutants displayed a reduction of over 10% in Q_{OFF} for the same activation protocol. This suggests that the mutation may be causing the stabilization of the VSD in an “activated-like” state.

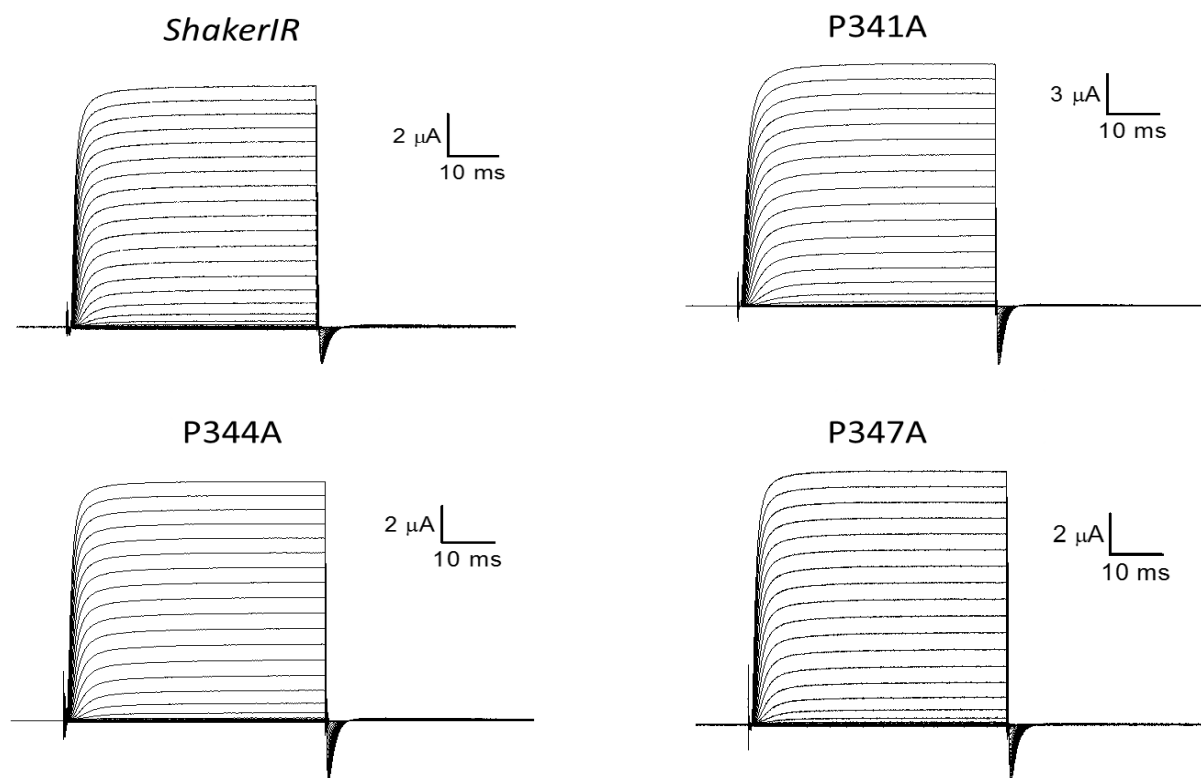


Figure 4. Ionic activation currents in ShakerIR constructs. Pulses were elicited from -120 mV to $+40 \text{ mV}$ in 5 mV steps for ShakerIR and S3-S4 loop proline-to-alanine mutants with a holding potential of -90 mV .

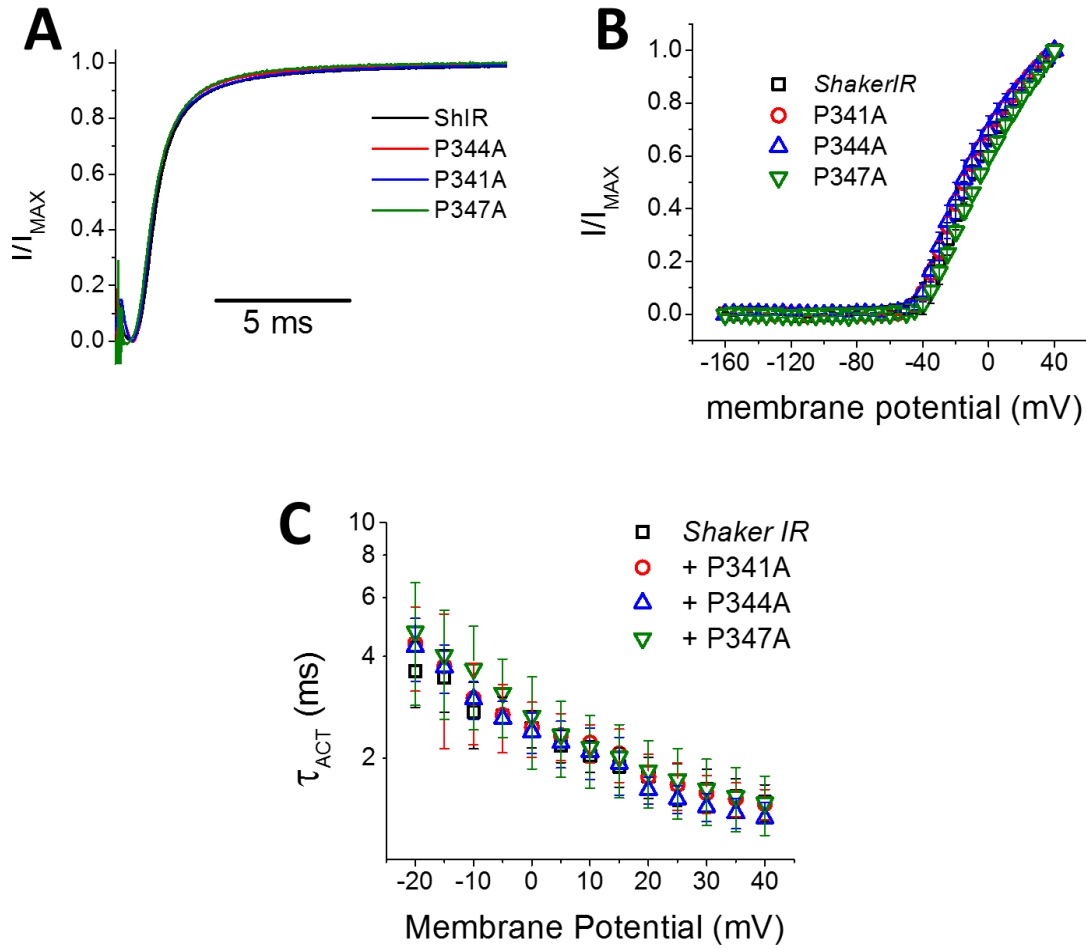


Figure 5. Kinetics of channel activation. Detail of the activation current was measured from pulses ranging from -120 mV to +40 mV in 5 mV steps in ShakerIR and the proline-to-alanine mutants (A). The graph illustrates the ratio of total current to maximal current as a function of time (ms). The ratio of total current to maximal current (B) as a function of membrane potential (mV) illustrates the voltage dependence of activation for each of the ShakerIR constructs. Current in (B) was measured at the end of the 50 ms depolarizing step. The time constant of channel activation was obtained following a +40 mV pulse for 150 ms (C). The current after the activation step was fitted to a two-exponential function.

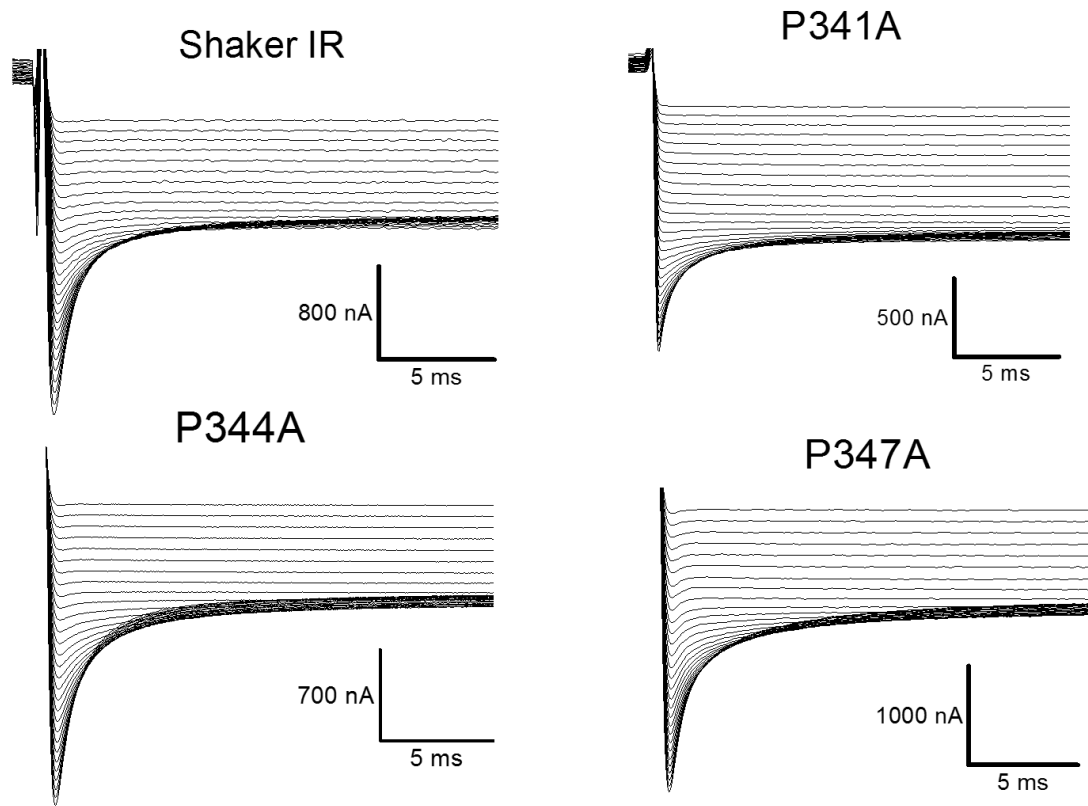


Figure 6. Ionic deactivation currents from ShakerIR and proline-to-alanine mutants. Following depolarization to +40 mV for 5000 ms, pulses were elicited from -140 mV to +20 mV in 5 mV steps for *ShakerIR* and S3-S4 loop proline-to-alanine mutants with a holding potential of -90 mV. The proline-to-alanine mutants appear to deactivate slower than *ShakerIR*.

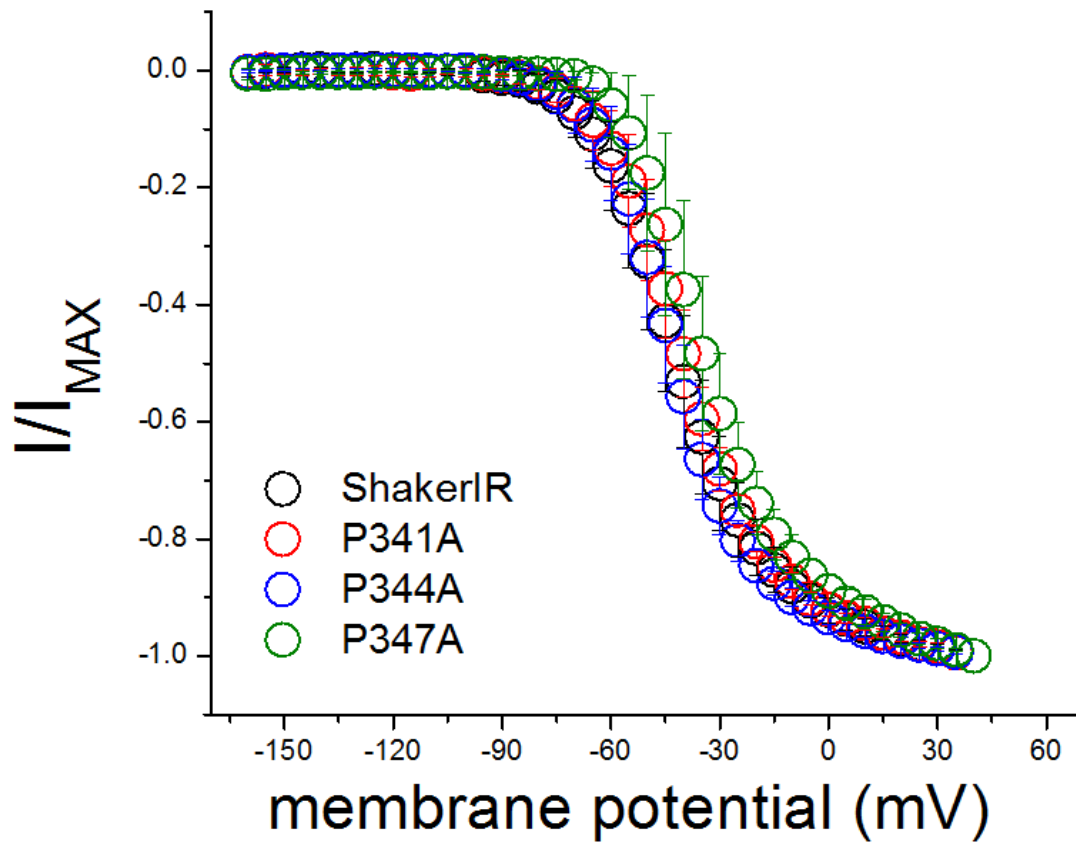


Figure 7. Voltage dependence of channel deactivation following relaxation.

After inducing relaxation with a pre-pulse of +40mV for 1000 ms, the ShakerIR and proline-to-alanine mutants were deactivated from -160 mV to +40 mV. The voltage dependence of channel deactivation for ShakerIR ($n = 8$) and each of the mutants P341A ($n = 4$), P344A ($n = 5$), P347A ($n = 4$) is not shifted.

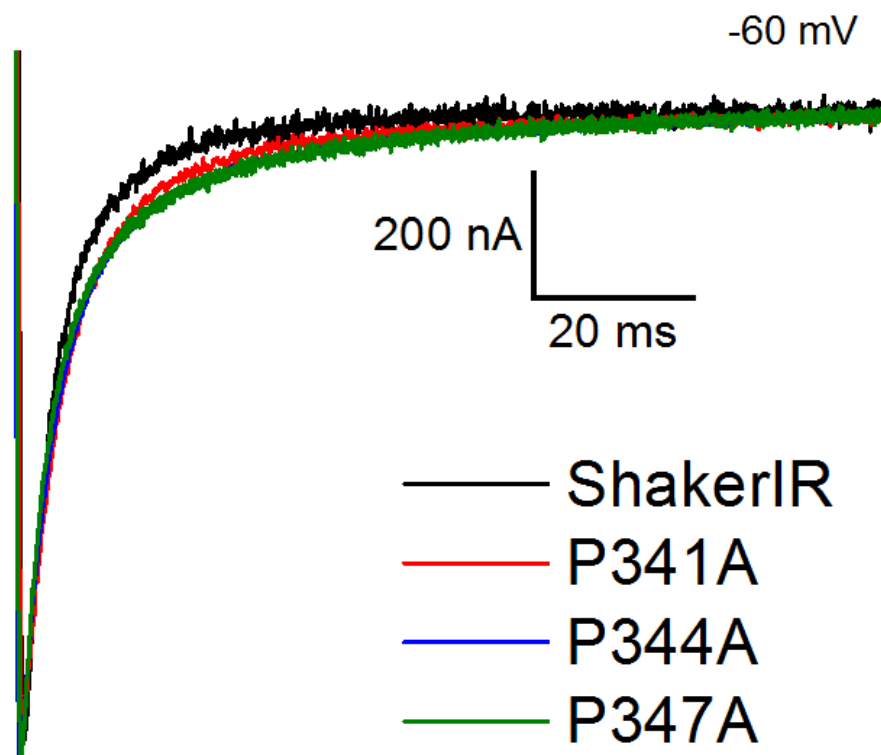


Figure 8. Deactivation current kinetics in detail. The normalized deactivation currents at -60 mV for *ShakerIR* and each of the proline-to-alanine mutants was plotted after a depolarizing pre-pulse to +40 mV for 1000 ms. For each of the proline-to-alanine mutants, the deactivation following the pre-pulse appeared slower compared to that of *ShakerIR*.

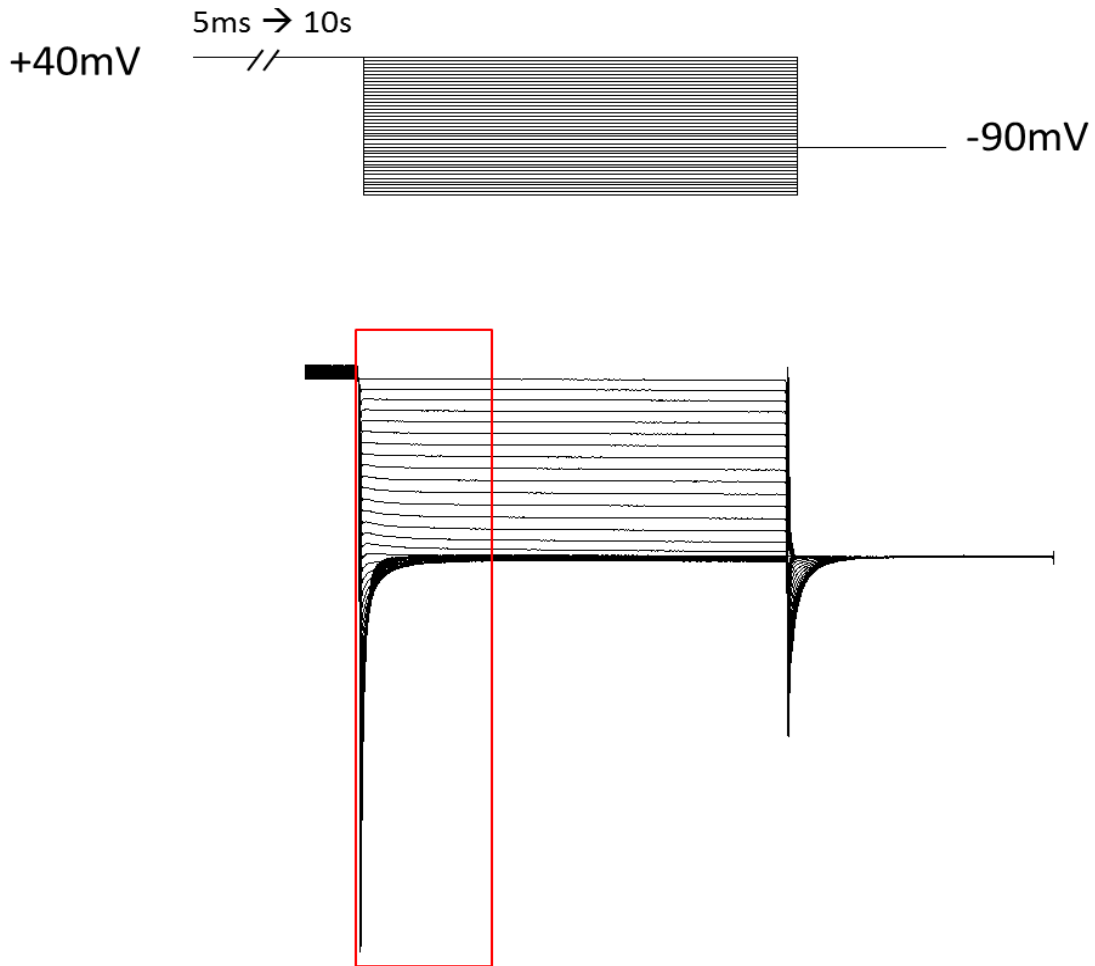


Figure 9. Relaxation voltage clamp protocol. Relaxation was measured in *Xenopus oocytes* using a cut-open voltage clamp setup. The protocol for the induction of relaxation began with a depolarizing pre-pulse to +40 mV for durations ranging between 5 ms and 10 s, followed by a deactivation step ranging from approximately -160 mV to +40 mV. The holding potential was -90 mV. The deactivation of the channel, indicated in the red box, was fitted to a two-exponential equation to obtain a τ_{DEAC} .

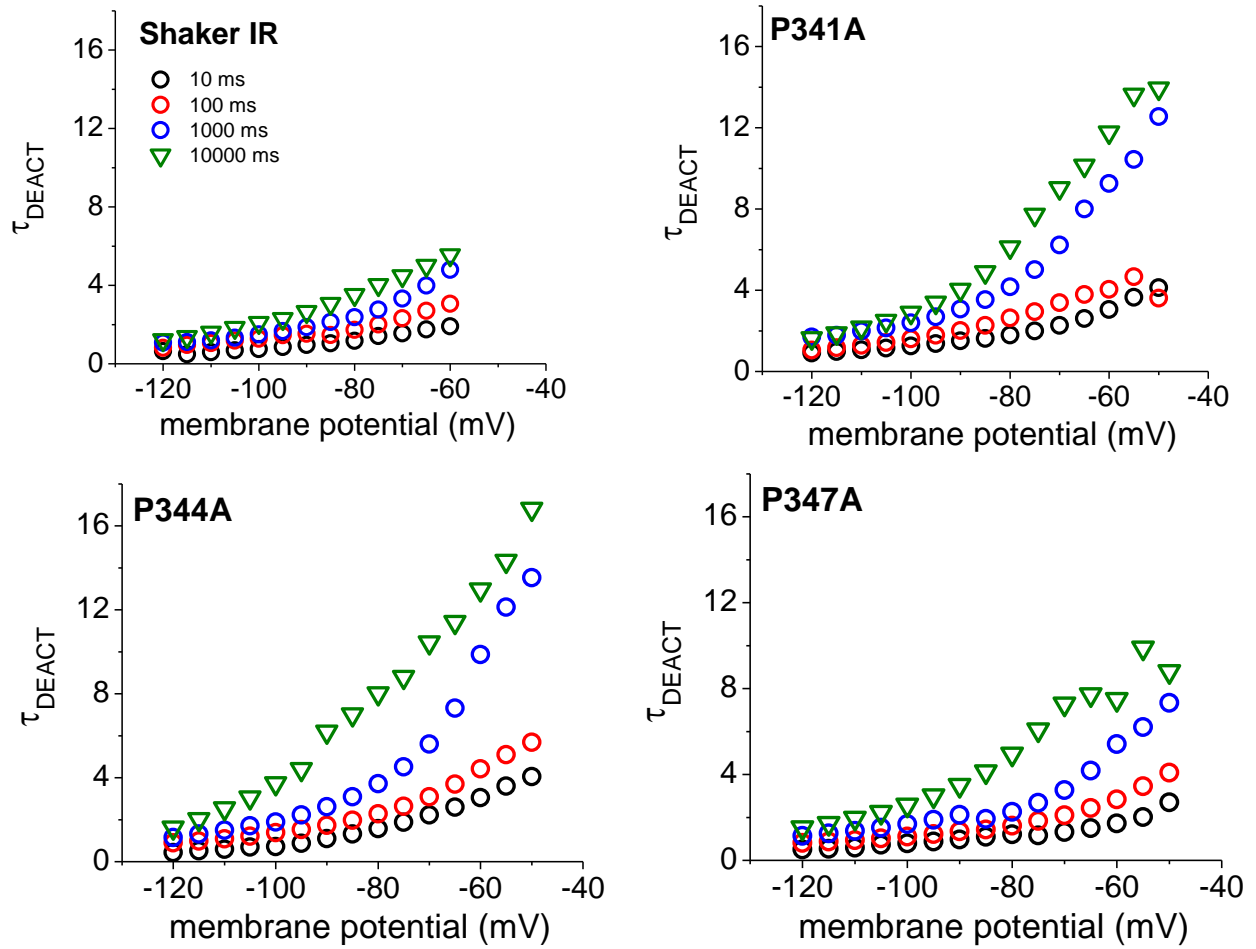


Figure 10. Weighted average time constant of deactivation, τ_{DEACT} , following depolarizing pre-pulse of varying duration. A pre-pulse of +40 mV was applied to ShakerIR ($n = 1$) and each of the proline to alanine mutants ($n = 1$) for durations varying between 10 ms and 10 s. Note in each of the mutants the sharp increase in τ_{DEACT} for longer pre-pulse durations of 1000 ms and 10 s.

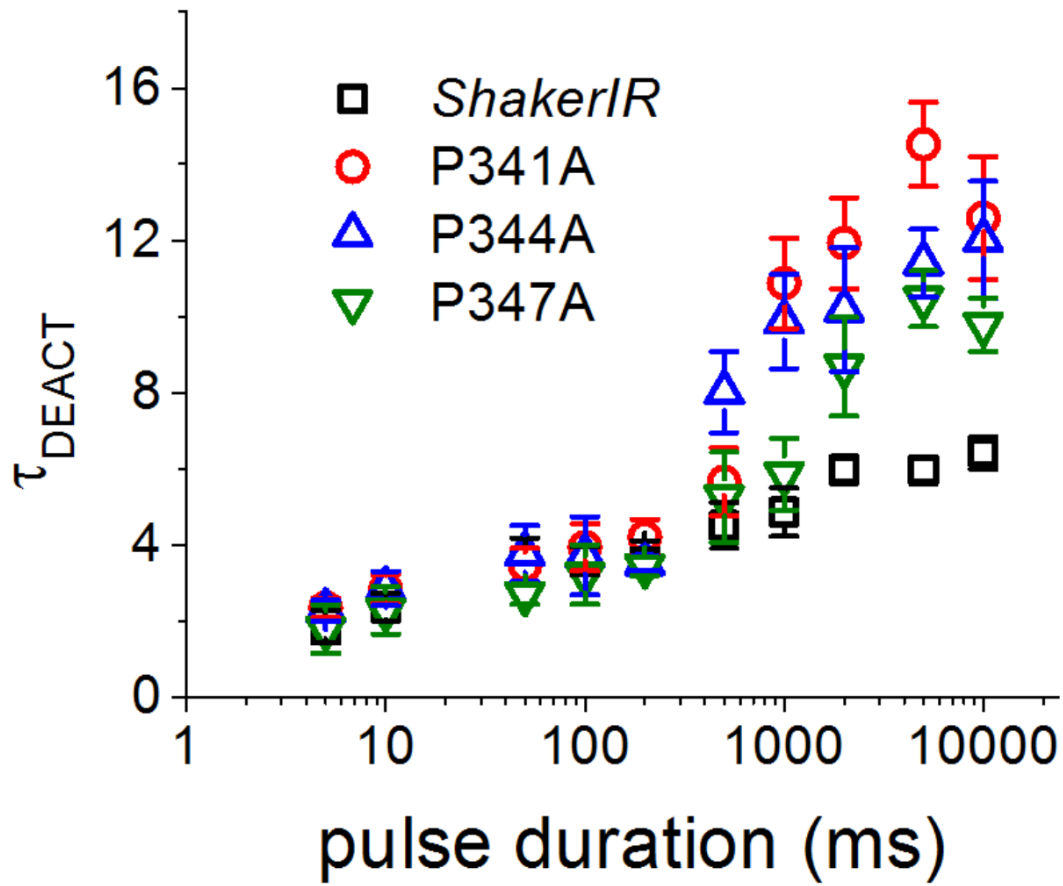
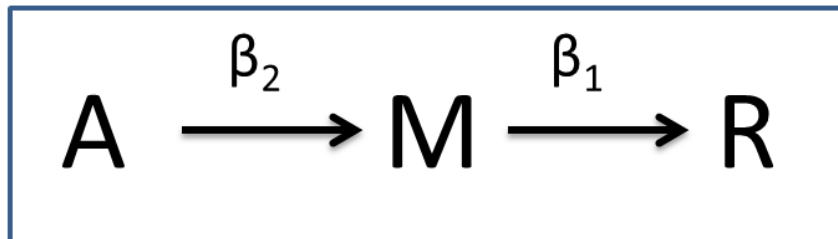
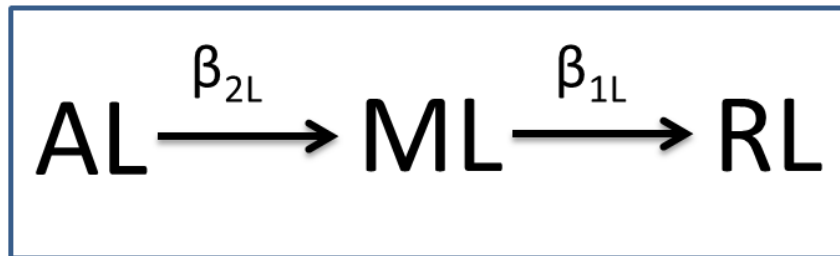


Figure 11. Weighted average time constant of deactivation, τ_{DEAC} , as a function of depolarizing pre-pulse duration. A pre-pulse of 40 mV was applied to *ShakerIR* ($n = 6$), P341A ($n = 7$), P344A ($n = 6$), and P347A ($n = 7$), for durations varying between 5 ms and 10 s. The weighted τ_{DEAC} was calculated at -60 mV using a two-exponential fit. Note the sharp increase in τ_{DEAC} for mutants at longer pre-pulse durations ($p < 0.05$).

Non-Relaxed



Relaxation



Relaxed

Figure 12. Voltage Sensor Relaxation Transition Model. Describes the deactivation of the VSD in two parallel conformations, the non-relaxed and the relaxed state. Each transition of the VSD during deactivation at negative potentials is governed by a rate constant, β .

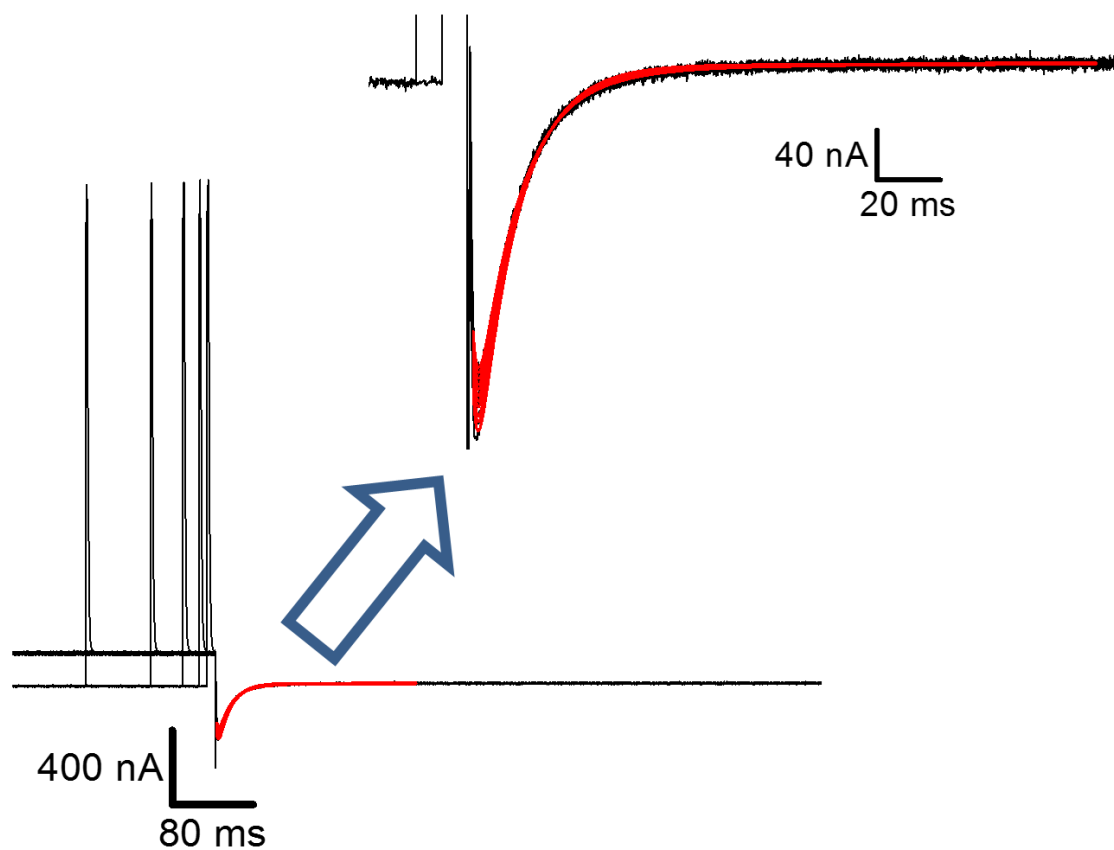


Figure 13. W434F gating current fitting. Example of a set of gating current traces (black) fit to the model for OFF-gating currents (red). The inset show details of the fitting.

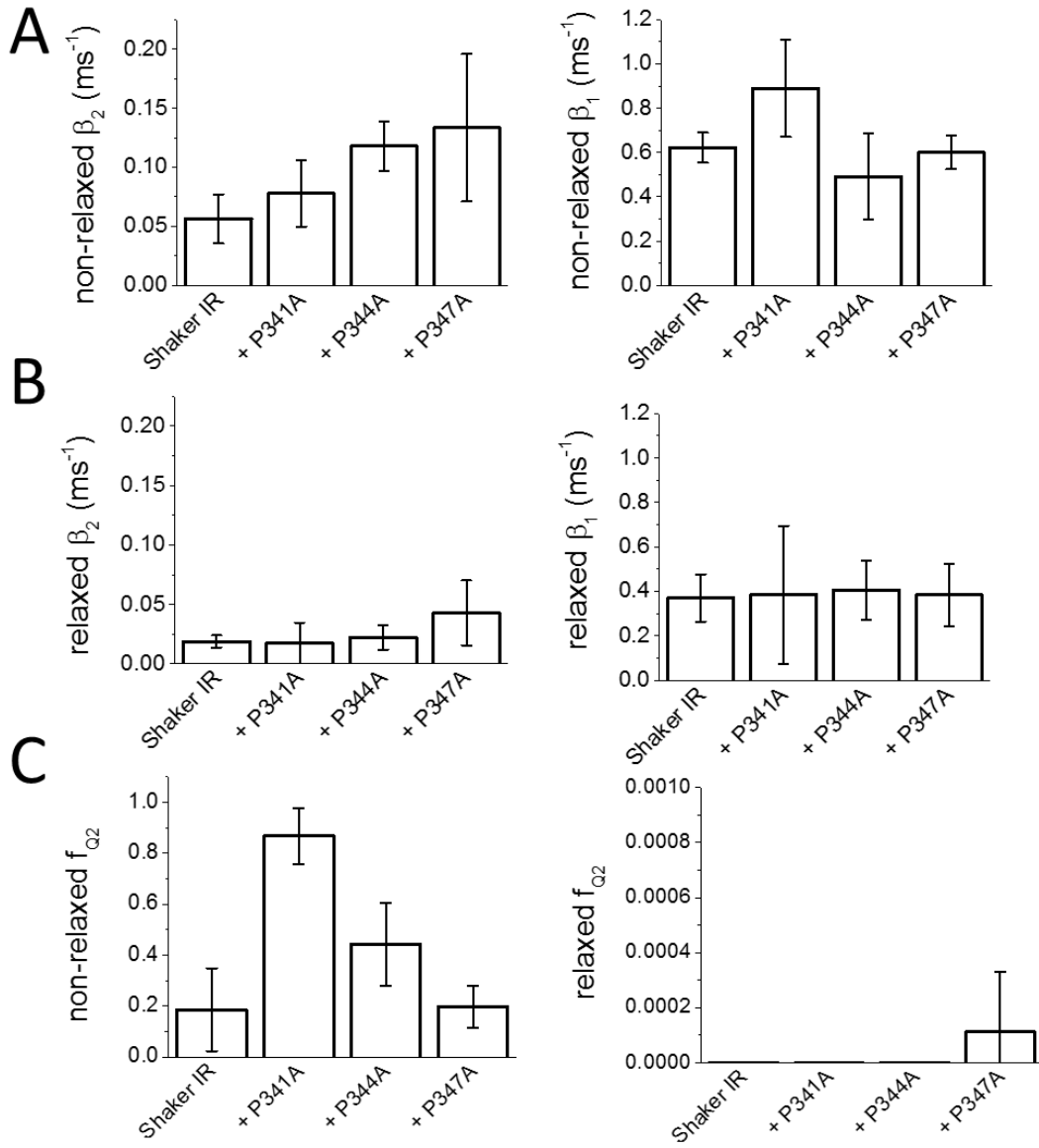


Figure 14. Off gating current kinetics. Using Shaker W434F, gating currents for Shaker ($n = 4$), P341A ($n = 4$), P344A ($n = 5$), and P347A ($n = 4$) were fitted to the solution for the differential equation (see methods) describing the OFF-gating current. (A) and (B) describe the rates off the OFF-gating currents in the non-relaxed and relaxed states, according to the model in Figure 12. (β_{11} : $p < 0.05$, β_{12} : $p < 0.05$, f_{12} : $p < 0.05$, β_{21} : $p < 0.09$, β_{22} : $p < 0.14$, f_{22} : $p < 0.39$)

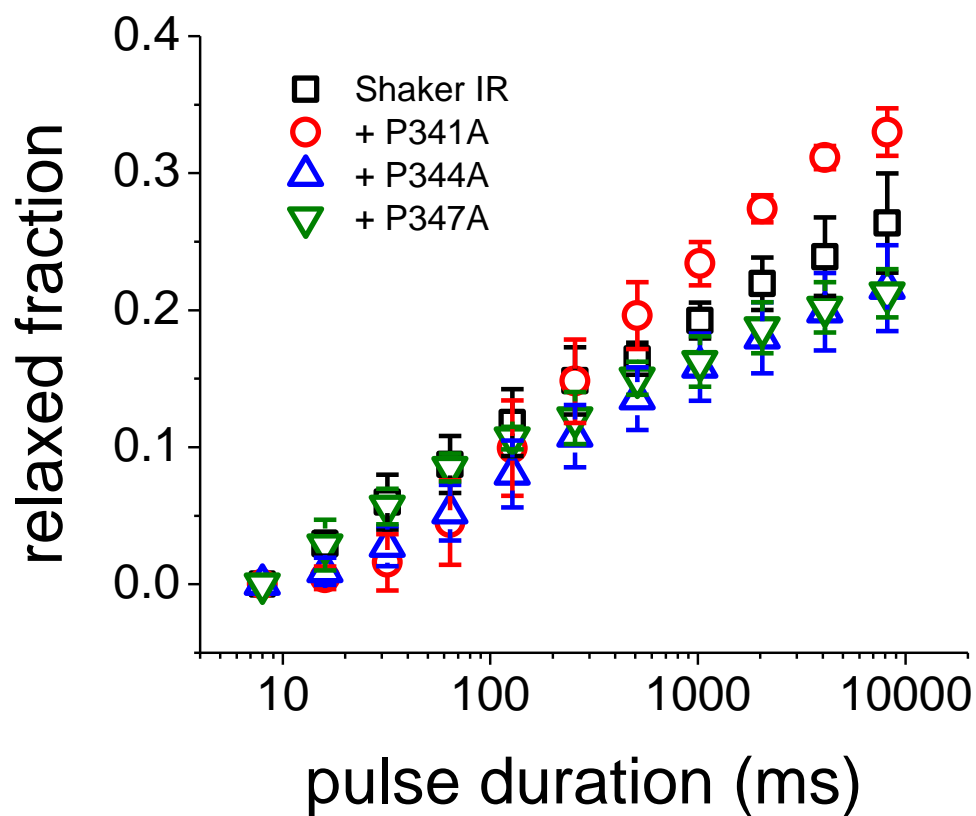


Figure 15. Fraction of voltage sensors in the relaxed state. The fraction of voltage sensors in the relaxed state increased as a function of the initial depolarizing pulse duration. The proline-to-alanine mutation at position 341 ($n = 4$) demonstrated the largest fraction of relaxed VSDs at longer pulse durations. There appeared to be no difference between the fraction of relaxed VSDs of Shaker ($n = 4$), P344A ($n = 5$), and P347A ($n = 4$).

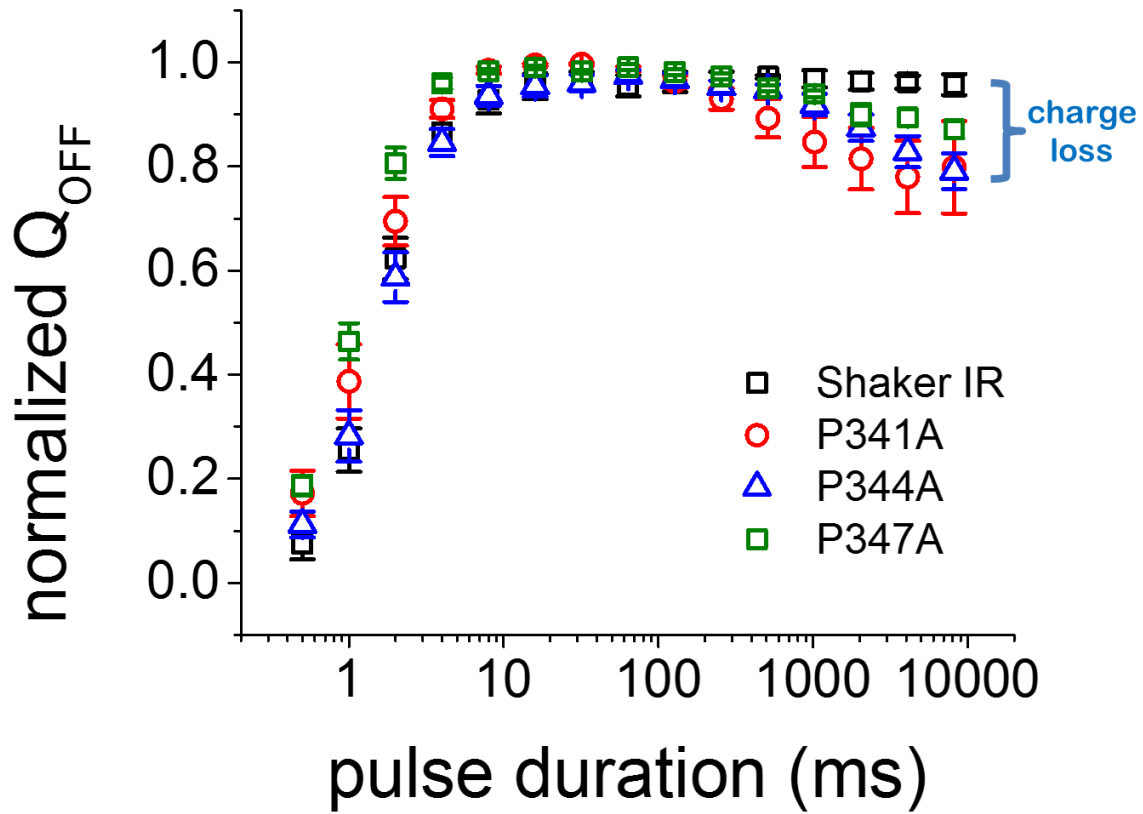


Figure 16. Normalized off gating charge during relaxation. Prolonged depolarization caused an apparent decrease in the total gating charge integrated from OFF-gating currents. This indicates that a fraction of the OFF-charge in the mutants is moving too slowly thus, the currents produced cannot be resolved even when integrating for 300 ms. *Shaker* W434F ($n = 4$), P341A ($n = 4$), P344A ($n = 5$), and P347A ($n = 4$)

Discussion and Conclusion

In general, there did not appear to be a significant difference in channel activation between the three proline-to-alanine mutations and the background construct, *ShakerIR*. The three mutants and *ShakerIR* had a nearly identical voltage dependence of activation at -40 mV (Fig. 5B). There appeared to be no difference between the τ_{ACT} for *ShakerIR* and the τ_{ACT} for the proline-to-alanine mutants (Fig. 5C). We conclude from these data that the mutation of individual S3-S4 loop prolines 341, 344, and 347 is well tolerated in *ShakerIR*, resulting in no change in channel expression, and seems to have no effect on the kinetics or voltage dependence of activation of *ShakerIR*.

The data indicate the significance of the proline residues within the S3-S4 linker helix in the modulation of voltage sensor relaxation. For the *ShakerIR* and the proline-to-alanine mutants, the τ_{DEACT} increased as membrane potential became more positive (Fig. 10). Additionally, τ_{DEACT} increased as a function of the depolarizing pre-pulse duration, suggesting that the open state was stabilized during the pre-pulse (Fig. 11). At short pre-pulse durations of 200 ms and less, there is no differentiation between the time constant of *ShakerIR* and the time constants of the three mutants (Fig. 11). However, at pre-pulse durations of 500 ms and greater, there is a large shift in the τ_{DEACT} of each mutant

compared to the τ_{DEACT} of *ShakerIR*. After a 10 s pulse to +40 mV, the τ_{DEACT} for *ShakerIR* was $6.42 \text{ ms} \pm 0.4245$ at -60 mV. Under the same conditions, the τ_{DEACT} for the P341A mutation ($12.59 \text{ ms} \pm 1.61$), P344A mutation ($12.02 \text{ ms} \pm 1.54$), and P347 mutation ($9.79 \text{ ms} \pm 0.70$) were comparatively higher. From these data, it can be inferred that at pre-pulse durations of 200 ms and less, the voltage sensor undergoes activation and the pore is stabilizing. Thus, in this fast phase of $I_{\text{DEACT}}-t$ curve there will be no difference in the deactivation time constants between the wildtype and proline-to-alanine mutants. However, at longer pre-pulse durations, the voltage sensor undergoes relaxation and enters the slow phase of $I_{\text{DEACT}}-t$ curve. While the τ_{DEACT} for Shaker does increase at longer pre-pulse durations, indicating relaxation, the τ_{DEACT} observed in the proline-to-alanine mutants are much slower (Fig. 11). This indicates that the stabilization of the open state, following relaxation, is greater in the mutant than for *ShakerIR*. Thus, these results seem to indicate that the mutant VSDs experience a deeper state of relaxation.

The effect of the mutations on relaxation in the gating charges is less clear. There appears to be no change in the kinetics of the gating charge during deactivation between *ShakerIR* and the proline-to-alanine W434F mutants (Fig. 14A,B). Relaxation is occurring in all of the *ShakerIR* constructs, since the rates of charge movement are slower in the relaxed state than in the non-relaxed state and the fraction of VSDs in the relaxed state is increasing with the depolarizing pulse duration (Fig. 15). However, the effect of the mutations on channel relaxation should likely be amplified in the VSD transition rates β_{2L} and β_{1L} , but interestingly there is no slowing down of the rates (Fig.14B).

Additionally, only the P341A mutation appears to have a significant effect on the fraction of voltage sensors in the relaxed state (Fig. 15), even though it has been demonstrated by the $I_{\text{DEACT}}-t$ curve that all three proline-to-alanine mutations have an apparent effect on relaxation (Fig. 11). The possibility arises then that we are unable to resolve the level of relaxation. This is based on the charge loss seen in the mutants at long depolarization times, when relaxation is known to occur (Labro et al., 2012; Lacroix et al., 2011). This charge loss is indicative of a very slow component, possibly increased relaxation of the mutant channels that is preventing the full charge movement from being observed. Therefore, this charge movement is limiting the deactivation. This would explain why the kinetics of the transition rates do not change; the VSDs being observed are mostly in the non-relaxed state.

The apparent discrepancy between the gating current and ionic current data can be explained by the gating transitions of the VSD during relaxation. Since each channel requires the movement of four S4 segments to gate the pore, the S4 segment becomes a limiting factor. When the S4 segments are activated for a long period and enter the stable relaxed state, they force the pore into the open, conducting state until all four S4 segments return to the resting state. If just one single S4 segment does not return to the resting state, then the pore stays open. Our data seem to illustrate just that phenomenon. The W434F gating currents for all constructs show that the VSDs occupy predominately the resting state, with approximately 2% of the *ShakerIR* and 10% of the mutant VSDs in the relaxed state at long pre-pulse durations (Fig. 16). This small percentage of VSDs in

the relaxed state is sufficient enough to increase the time constant of deactivation for the channel conductance. The difference in the percentage of VSDs in the relaxed state between the *ShakerIR* and proline-to-alanine mutants is evident in the significantly slower deactivation time constants for the mutants (Fig. 11). The reason that the gating currents are not slower is because the actual percentage of VSDs in the relaxed state is so little that the slowing cannot be resolved (Fig. 16).

The initial hypothesis is centered on the assumption that part of the S3-S4 linker is folded into an alpha-helix and likely functions as a “transmission line” for electromechanical energy between the S4 segment and the rest of the VSD. As the S4 segment moves during depolarization of the membrane, the S3-S4 linker will couple the movement of the S4 segment to the rest of the voltage-sensing domain. If the linker is flexible, the electromechanical energy from the S4 segment movement will be inefficiently transmitted to the rest of the VSD segments and will be dissipated by the linker itself. In contrast, if the linker is rigid, the S4 segment movement would be coupled to the S3 segment and the rest of the VSD. In this scenario, a large fraction of electromechanical energy will be stored in the VSD. The eventual dissipation of this energy will result in the stabilization of the VSD in a new conformation, the relaxed state.

The presence of proline in the S3-S4 linker may serve as helix-breaking points, conferring a level of flexibility within this region (Fig 1). In this view, proline residues in *ShakerIR* likely act as hinges within the S3-S4 loop. Arguably, mutating these prolines to a residue that favors alpha-helical folding, e.g. alanine, may transform the S3-S4 linker

into a more rigid body which would increase the coupling the S4 to the S3 segment. The S4 would effectively push with more force on the rest of the VSD due to the more rigid S3-S4 loop. Part of this effect can be seen in the P341A and P344A mutants on gating current deactivation. A large amount of charge is moved in the first transition step from *A* to *M* in these mutants, indicating that the alanine mutation is creating some stress on the S4 segment during deactivation (Fig 14C). The increased stress would lead to more S4 segment movement and thus more gating charge movement. This greater pushing force would also mean the conformational change of the VSD is greater and a deeper state of relaxation will occur. A greater amount of energy will therefore be needed to return the VSD to the resting state. This effect is illustrated in the significant increase in the τ_{DEACT} .

The data presented here supports the model that is proposed for VSD transition to relaxation. In the model, a resting VSD will transition to an intermediate state then an active state after depolarization. This active state is energetically unstable, and the VSD will then transition to an active-relaxed state. Following repolarization, the VSD will transition from active-relaxed to an intermediate-relaxed state then a resting-relaxed and finally back to the resting state. Under short depolarization times, 200 ms or less as indicated in Figure 11, the transition from resting to active state is too quick for relaxation to occur. However after a pre-pulse period of 500 ms or longer, the voltage sensor reaches the active state and remains there long enough to reach the active-relaxed state. It is significant that the mutation did not affect the activation kinetics of the channel (Fig.5). Had the transition from resting to active state differed under mutation of proline-

to-alanine, then the mutation's effect on relaxation would be invalid. The relaxed state depends on the VSD reaching the active state, and the proline-to-alanine mutation has shown that its effect is solely on the relaxation of the VSD.

Final remarks

5.1: Future Directions

Future directions of this project will attempt to measure the voltage dependency of the gating currents for *ShakerIR* and the proline-to-alanine mutants as a function of the pre-pulse duration. Additionally, a triple mutant of the S3-S4 loop that replaces P341, P344, and P347 with alanine should be constructed. The mutation of all three prolines at once would likely confer an even greater rigidity to the S3-S4 loop, resulting in a further state of relaxation than a single proline-to-alanine mutation. In order to further support the effect of the proline-to-alanine mutations on VSD relaxation, site-directed fluorometry of the S4 movement would need to be correlated with I_{OFF} and I_{DEACT} slowing. This would map the S4 segment movement in relation to the kinetics of the VSD and pore.

5.2: On the physiological role of VSD relaxation

At physiological concentrations, the driving force of the potassium ions is typically between -60 mV and -80 mV. In excitable cells, the activation of a potassium selective conductance is needed to repolarize the plasma membrane following an action potential. Since the era of Hodgkin and Huxley, when it was first demonstrated, the orchestrated actions of sodium- and potassium-selective conductance give rise to action potentials in

excitable cells. In general, a rapidly-activated sodium conductance drives the depolarization of the membrane, followed later by the delayed activation of a voltage-gated potassium conductance, bringing the membrane potential back to its resting voltage. Thus, the activity of the potassium channels is critical for resetting the electric machinery in order to generate new action potentials.

Small changes in the voltage dependence of potassium channels may have a tremendous impact on the generation of electrical signals in excitable cells. It has been shown that changes of as little as -2 mV in the voltage dependence for potassium conductance activation can abrogate the generation of action potentials trains in model systems (Borjesson and Elinder, 2008). Thus, VSD relaxation may have a significant impact in cellular excitability.

To date, our understanding of the physiological relevance of VSD relaxation in electrical activity of excitable cells is incomplete. This inherent VSD process of relaxation can potentially cause disease or abnormal phenotypes due to alterations of normal channel gating. In cardiac diseases where sodium and potassium channels are necessary for regulation of action potential duration, the process of relaxation could be potentially fatal. Potassium channels play a significant role in repolarization of the cardiac myocytes, which occurs in three distinct phases (Sanguinetti and Tristani-Firouzi, 2006). The first phase of repolarization is rapid, followed by a second phase plateau. The second phase acts as an anti-arrhythmic defense mechanism by preventing premature excitation of the cardiac myocytes. Phase 3 ends the action potential and brings the

membrane potential back to baseline via hERG channel rapid-delayed potassium current (Sanguinetti and Tristani-Firouzi, 2006). Alterations of the hERG gating can abolish its rapid inactivation, thus conferring a gain-of-function mutation. This increased outward repolarizing current has been shown to shorten the QT interval and cause ventricular fibrillation and sudden death (Sanguinetti and Tristani-Firouzi, 2006). In gain-of-function sodium channelopathies, pore inactivation is reduced or eliminated, resulting in continuous inward current (Sanguinetti and Tristani-Firouzi, 2006). This results in long QT syndrome, a cardiac arrhythmia that could lead to sudden death. In regards to VSD relaxation, the implication is that significant time spent in the relaxed state keeps the channel open for abnormally long periods of time, leading to increased current conductance. Mutations that increase VSD relaxation could likely confer a gain-of-function in current conductance that disrupts the delicate balance of ionic currents.

Literature Cited

Literature Cited

- Aggarwal, S.K., and R. MacKinnon. 1996. Contribution of the S4 segment to gating charge in the Shaker K⁺ channel. *Neuron*. 16:1169-1177.
- Akemann, W., A. Lundby, H. Mutoh, and T. Knopfel. 2009. Effect of voltage sensitive fluorescent proteins on neuronal excitability. *Biophysical journal*. 96:3959-3976.
- Armstrong, C.M., and F. Bezanilla. 1973. Currents related to movement of the gating particles of the sodium channels. *Nature*. 242:459-461.
- Batulan, Z., G.A. Haddad, and R. Blunck. 2010. An intersubunit interaction between S4-S5 linker and S6 is responsible for the slow off-gating component in Shaker K⁺ channels. *The Journal of biological chemistry*. 285:14005-14019.
- Bezanilla, F. 2000. The voltage sensor in voltage-dependent ion channels. *Physiological reviews*. 80:555-592.
- Bezanilla, F. 2005. Voltage-gated ion channels. *IEEE transactions on nanobioscience*. 4:34-48.
- Bezanilla, F. 2008a. How membrane proteins sense voltage. *Nature reviews. Molecular cell biology*. 9:323-332.
- Bezanilla, F. 2008b. Ion channels: from conductance to structure. *Neuron*. 60:456-468.
- Bezanilla, F., and C.M. Armstrong. 1974. Gating currents of the sodium channels: three ways to block them. *Science*. 183:753-754.
- Bezanilla, F., M.M. White, and R.E. Taylor. 1982. Gating currents associated with potassium channel activation. *Nature*. 296:657-659.
- Borjesson, S.I., and F. Elinder. 2008. Structure, function, and modification of the voltage sensor in voltage-gated ion channels. *Cell biochemistry and biophysics*. 52:149-174.
- Bruening-Wright, A., and H.P. Larsson. 2007. Slow conformational changes of the voltage sensor during the mode shift in hyperpolarization-activated cyclic-nucleotide-gated channels. *The Journal of neuroscience : the official journal of the Society for Neuroscience*. 27:270-278.

- Gonzalez, C., E. Rosenman, F. Bezanilla, O. Alvarez, and R. Latorre. 2000. Modulation of the Shaker K(+) channel gating kinetics by the S3-S4 linker. *The Journal of general physiology*. 115:193-208.
- Gonzalez, C., E. Rosenman, F. Bezanilla, O. Alvarez, and R. Latorre. 2001. Periodic perturbations in Shaker K⁺ channel gating kinetics by deletions in the S3-S4 linker. *Proceedings of the National Academy of Sciences of the United States of America*. 98:9617-9623.
- Haddad, G.A., and R. Blunck. 2011. Mode shift of the voltage sensors in Shaker K⁺ channels is caused by energetic coupling to the pore domain. *The Journal of general physiology*. 137:455-472.
- Halaszovich, C.R., D.N. Schreiber, and D. Oliver. 2009. Ci-VSP is a depolarization-activated phosphatidylinositol-4,5-bisphosphate and phosphatidylinositol-3,4,5-trisphosphate 5'-phosphatase. *The Journal of biological chemistry*. 284:2106-2113.
- Hodgkin, A.L., and A.F. Huxley. 1952a. The components of membrane conductance in the giant axon of Loligo. *The Journal of physiology*. 116:473-496.
- Hodgkin, A.L., and A.F. Huxley. 1952b. A quantitative description of membrane current and its application to conduction and excitation in nerve. *The Journal of physiology*. 117:500-544.
- Kanevsky, M., and R.W. Aldrich. 1999. Determinants of voltage-dependent gating and open-state stability in the S5 segment of Shaker potassium channels. *The Journal of general physiology*. 114:215-242.
- Keynes, R.D., and E. Rojas. 1973. Characteristics of the sodium gating current in the squid giant axon. *The Journal of physiology*. 233:28P-30P.
- Kurokawa, T., S. Takasuga, S. Sakata, S. Yamaguchi, S. Horie, K.J. Homma, T. Sasaki, and Y. Okamura. 2012. 3' Phosphatase activity toward phosphatidylinositol 3,4-bisphosphate [PI(3,4)P₂] by voltage-sensing phosphatase (VSP). *Proceedings of the National Academy of Sciences of the United States of America*. 109:10089-10094.
- Kuzmenkin, A., F. Bezanilla, and A.M. Correa. 2004. Gating of the bacterial sodium channel, NaChBac: voltage-dependent charge movement and gating currents. *The Journal of general physiology*. 124:349-356.

- Labro, A.J., J.J. Lacroix, C.A. Villalba-Galea, D.J. Snyders, and F. Bezanilla. 2012. Molecular mechanism for depolarization-induced modulation of Kv channel closure. *The Journal of general physiology*. 140:481-493.
- Lacroix, J.J., and F. Bezanilla. 2011. Control of a final gating charge transition by a hydrophobic residue in the S2 segment of a K⁺ channel voltage sensor. *Proceedings of the National Academy of Sciences of the United States of America*. 108:6444-6449.
- Lacroix, J.J., and F. Bezanilla. 2012. Tuning the voltage-sensor motion with a single residue. *Biophysical journal*. 103:L23-25.
- Lacroix, J.J., A.J. Labro, and F. Bezanilla. 2011. Properties of deactivation gating currents in Shaker channels. *Biophysical journal*. 100:L28-30.
- Larsson, H.P., and F. Elinder. 2000. A conserved glutamate is important for slow inactivation in K⁺ channels. *Neuron*. 27:573-583.
- Long, S.B., E.B. Campbell, and R. Mackinnon. 2005a. Crystal structure of a mammalian voltage-dependent Shaker family K⁺ channel. *Science*. 309:897-903.
- Long, S.B., E.B. Campbell, and R. Mackinnon. 2005b. Voltage sensor of Kv1.2: structural basis of electromechanical coupling. *Science*. 309:903-908.
- Long, S.B., X. Tao, E.B. Campbell, and R. MacKinnon. 2007. Atomic structure of a voltage-dependent K⁺ channel in a lipid membrane-like environment. *Nature*. 450:376-382.
- Murata, Y., H. Iwasaki, M. Sasaki, K. Inaba, and Y. Okamura. 2005. Phosphoinositide phosphatase activity coupled to an intrinsic voltage sensor. *Nature*. 435:1239-1243.
- Murata, Y., and Y. Okamura. 2007. Depolarization activates the phosphoinositide phosphatase Ci-VSP, as detected in *Xenopus* oocytes coexpressing sensors of PIP₂. *The Journal of physiology*. 583:875-889.
- Noda, M., S. Shimizu, T. Tanabe, T. Takai, T. Kayano, T. Ikeda, H. Takahashi, H. Nakayama, Y. Kanaoka, N. Minamino, and et al. 1984. Primary structure of *Electrophorus electricus* sodium channel deduced from cDNA sequence. *Nature*. 312:121-127.
- Olcese, R., R. Latorre, L. Toro, F. Bezanilla, and E. Stefani. 1997. Correlation between charge movement and ionic current during slow inactivation in Shaker K⁺ channels. *The Journal of general physiology*. 110:579-589.

- Perozo, E., R. MacKinnon, F. Bezanilla, and E. Stefani. 1993. Gating currents from a nonconducting mutant reveal open-closed conformations in Shaker K⁺ channels. *Neuron*. 11:353-358.
- Piper, D.R., A. Varghese, M.C. Sanguinetti, and M. Tristani-Firouzi. 2003. Gating currents associated with intramembrane charge displacement in HERG potassium channels. *Proceedings of the National Academy of Sciences of the United States of America*. 100:10534-10539.
- Sanguinetti, M.C., and M. Tristani-Firouzi. 2006. hERG potassium channels and cardiac arrhythmia. *Nature*. 440:463-469.
- Schoppa, N.E., K. McCormack, M.A. Tanouye, and F.J. Sigworth. 1992. The size of gating charge in wild-type and mutant Shaker potassium channels. *Science*. 255:1712-1715.
- Seoh, S.A., D. Sigg, D.M. Papazian, and F. Bezanilla. 1996. Voltage-sensing residues in the S2 and S4 segments of the Shaker K⁺ channel. *Neuron*. 16:1159-1167.
- Shirokov, R., G. Ferreira, J. Yi, and E. Rios. 1998. Inactivation of gating currents of L-type calcium channels. Specific role of the alpha 2 delta subunit. *The Journal of general physiology*. 111:807-823.
- Shirokov, R., R. Levis, N. Shirokova, and E. Rios. 1992. Two classes of gating current from L-type Ca channels in guinea pig ventricular myocytes. *The Journal of general physiology*. 99:863-895.
- Sigg, D., E. Stefani, and F. Bezanilla. 1994. Gating current noise produced by elementary transitions in Shaker potassium channels. *Science*. 264:578-582.
- Swartz, K.J. 2008. Sensing voltage across lipid membranes. *Nature*. 456:891-897.
- Tabarean, I.V., and C.E. Morris. 2002. Membrane stretch accelerates activation and slow inactivation in Shaker channels with S3-S4 linker deletions. *Biophysical journal*. 82:2982-2994.
- Taglialatela, M., L. Toro, and E. Stefani. 1992. Novel voltage clamp to record small, fast currents from ion channels expressed in *Xenopus* oocytes. *Biophysical journal*. 61:78-82.
- Tempel, B.L., D.M. Papazian, T.L. Schwarz, Y.N. Jan, and L.Y. Jan. 1987. Sequence of a probable potassium channel component encoded at Shaker locus of *Drosophila*. *Science*. 237:770-775.

- Tombola, F., M.M. Pathak, and E.Y. Isacoff. 2006. How does voltage open an ion channel? *Annual review of cell and developmental biology*. 22:23-52.
- Vieira-Pires, R.S., and J.H. Morais-Cabral. 2010. 3(10) helices in channels and other membrane proteins. *The Journal of general physiology*. 136:585-592.
- Villalba-Galea, C.A. 2012. Voltage-Controlled Enzymes: The New JanusBifrons. *Frontiers in pharmacology*. 3:161.
- Villalba-Galea, C.A., F. Miceli, M. Taglialatela, and F. Bezanilla. 2009a. Coupling between the voltage-sensing and phosphatase domains of Ci-VSP. *The Journal of general physiology*. 134:5-14.
- Villalba-Galea, C.A., W. Sandtner, D. Dimitrov, H. Mutoh, T. Knopfel, and F. Bezanilla. 2009b. Charge movement of a voltage-sensitive fluorescent protein. *Biophysical journal*. 96:L19-21.
- Villalba-Galea, C.A., W. Sandtner, D.M. Starace, and F. Bezanilla. 2008. S4-based voltage sensors have three major conformations. *Proceedings of the National Academy of Sciences of the United States of America*. 105:17600-17607.

VITA

W. Everett Fox was born in Charlotte, NC on June 29, 1988. He graduated from Myers Park High School in Charlotte in 2007. He went on to receive a B.S. in Biology from the University of North Carolina, Chapel Hill, in 2011. After completing his undergraduate study, he pursued a Master's of Science in Physiology and Biophysics from Virginia Commonwealth University School of Medicine. After completing the Master's program, he hopes to go on to medical school and become a physician.